



# Field Trip Guide Book - P42

Florence - Italy  
August 20-28, 2004

*Volume n° 5 - from P37 to P54*

## **32<sup>nd</sup> INTERNATIONAL GEOLOGICAL CONGRESS**

### **GEOLOGY AND VOLCANISM OF STROMBOLI, LIPARI, AND VULCANO (AEOLIAN ISLANDS)**



*Leader: R. De Rosa*

*Associate Leaders: N. Calanchi, P.F. Dellino,  
L. Francalanci, F. Lucchi, M. Rosi,  
P.L. Rossi, C.A. Tranne*

**Post-Congress**

**P42**

*The scientific content of this guide is under the total responsibility of the Authors*

*Published by:*

**APAT – Italian Agency for the Environmental Protection and Technical Services - Via Vitaliano  
Brancati, 48 - 00144 Roma - Italy**



**APAT**  
Italian Agency for Environment  
Protection and Technical Services

*Series Editors:*

**Luca Guerrieri, Irene Rischia and Leonello Serva (APAT, Roma)**

*English Desk-copy Editors:*

**Paul Mazza (Università di Firenze), Jessica Ann Thonn (Università di Firenze), Nathalie Marlène  
Adams (Università di Firenze), Miriam Friedman (Università di Firenze), Kate Eadie (Freelance  
independent professional)**

*Field Trip Committee:*

**Leonello Serva (APAT, Roma), Alessandro Michetti (Università dell'Insubria, Como), Giulio Pavia  
(Università di Torino), Raffaele Pignone (Servizio Geologico Regione Emilia-Romagna, Bologna) and  
Riccardo Polino (CNR, Torino)**

*Acknowledgments:*

**The 32<sup>nd</sup> IGC Organizing Committee is grateful to Roberto Pompili and Elisa Brustia (APAT, Roma)  
for their collaboration in editing.**

*Graphic project:*

**Full snc - Firenze**

*Layout and press:*

**Lito Terrazzi srl - Firenze**



**32<sup>nd</sup> INTERNATIONAL  
GEOLOGICAL CONGRESS**

**GEOLOGY AND VOLCANISM  
OF STROMBOLI, LIPARI, AND  
VULCANO (AEOLIAN ISLANDS)**

**AUTHORS:**

*R. De Rosa<sup>1</sup>, N. Calanchi<sup>2</sup>, P.F. Dellino<sup>3</sup>, L. Francalanci<sup>4</sup>, F. Lucchi<sup>2</sup>,  
M. Rosi<sup>5</sup>, P.L. Rossi<sup>2</sup>, C.A. Tranne<sup>2</sup>*

*<sup>1</sup>Università della Calabria, Dipartimento di Scienze della Terra, Arcavacata di Rende,  
Cosenza - Italy*

*<sup>2</sup>Università di Bologna, Dipartimento di Scienze della Terra e Geologico-Ambientali,  
S. Donato, Bologna - Italy*

*<sup>3</sup>Università di Bari, Dipartimento geomineralogico, Bari - Italy*

*<sup>4</sup>Università di Firenze, Dipartimento di Scienze della Terra, Firenze - Italy*

*<sup>5</sup>Università di Pisa, Dipartimento di Scienze della Terra, Pisa - Italy*

**Florence - Italy  
August 20-28, 2004**

**Post-Congress**

**P42**

Front Cover:  
*A panoramic view of North Vulcano as seen  
from the Island of Lipari*

Leader: R. De Rosa

Associate Leaders: N. Calanchi, P.F. Dellino, L. Francalanci, F. Lucchi, M. Rosi, P.L. Rossi, C.A. Tranne

## Introduction

The Aeolian island arc represents a unique geological area, very well known all around the world as the site of some unusual volcanic activities and related deposits. Therefore, the first aim of this field trip will be to observe the two still active volcanic apparatus of Stromboli and Vulcano, where the typical “strombolian” and “vulcanian” eruptive styles have been described. Moreover, well-known volcanic deposits, such as the obsidian lava flows of Rocche Rosse and the pumiceous pyroclastics of Monte Guardia, will be shown on the Island of Lipari. The detailed analysis of the structural and textural features of some well-documented pyroclastics and lavas will be focused on, with the aim of acknowledging the processes governing the eruptive activity. The deposits related to low-medium energy eruptive dynamics of acid and basic magmas (strombolian, surtseyane, and vulcanian), that characterize the younger explosive eruptions of the Aeolian volcanoes, will be analyzed in detail. The wide variability of pyroclastic deposits that are present in Stromboli, Vulcano, and Lipari, and the broad compositional spectrum of emitted products, offer the possibility of analyzing the depositional facies of an adequate number of eruptions. Particular emphasis will be given to the reconstruction of the transportation and emplacement mechanisms of pyroclastic deposits. For some well-documented eruptive sequences, the quantitative assessment of hazard will be proposed. Furthermore, special attention will be devoted to the observation of ancient marine deposits (on Lipari, Salina, and Filicudi), indicating the complex relationships between volcanic activity and Late Quaternary eustatic fluctuations. Stratigraphical relationships between volcanics and raised ancient shorelines will be carefully described, showing the complex interaction between “local” volcanic and “global” Late-Quaternary eustatic events in the geological evolution of this volcanic apparatus.

## Regional geological setting

The volcanoes of the Aeolian Archipelago, and the associated volcanic seamounts, form a ring-shaped structure (Beccaluva et al., 1985), around the subsiding Marsili basin (1.8-0.2 Ma; Savelli, 2000) and Marsili seamount (0.7Ma-active; Marani and Trua, 2002) (Figs. 1).

The ring-shaped structure (the Aeolian Arc) consists



Figure 1 - Location of the Aeolian volcanic islands and associated seamounts.

of seven main islands (Alicudi, Filicudi, Salina, Lipari, Vulcano, Panarea, and Stromboli), and seven minor seamounts emplaced on a 15-20 km thinned continental crust (the Calabrian Arc) (Ventura et al., 1999).

In the light of structural, seismological, and geochemical data (De Astis et al., 2003), the Aeolian volcanism may be divided into three main structural/volcanological sectors (Fig. 2):

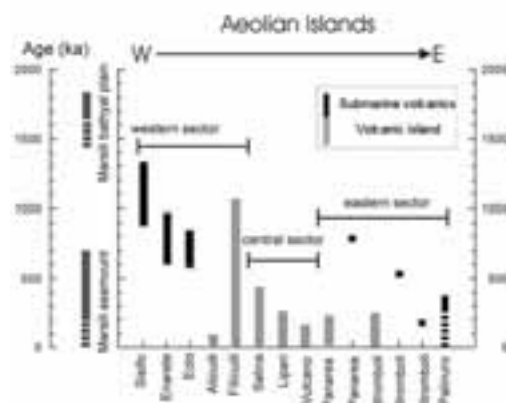


Figure 2 - Temporal evolution of the volcanism of the Aeolian area, based on the available geochronological data. From De Astis et al. (2003).

a) A western sector, which extends from the Glauco seamount to the Alicudi and Filicudi Islands. In this sector, the volcanism developed between 1.3 Myr and 30-40 kyr (Beccaluva et al., 1982; 1985; Santo et al.,

1995; De Rosa et al., 1993a). A WNW-ESE striking fault system (“Sisifo-Alicudi” system), characterized the tectonics of this area (Calanchi et al., 1995b).

b) A central sector, which includes the islands of Salina, Lipari and Vulcano. Here, the volcanism started at 0.4 Ma (Beccaluva et al., 1985), and it was still active at Lipari (580 AD) and Vulcano (1888-90 AD); at Salina, the last eruption occurred at 13 ka (Keller, 1980). Fumaroles, hot springs and shallow seismicity characterize large submarine and on-land areas (Gamberi et al., 1997). A NNW-SSE striking fault system (“Tindari-Letojanni” system, hereafter TL) affects the volcanoes of this central sector. These volcanoes are aligned along a NNW-SSE-striking structural depression (Barberi et al., 1994). The TL fault system represents the northern tip of the larger scale Malta escarpment fault system (Ghisetti, 1979; Continisio et al., 1997; Lanzafame and Bousquet, 1997).

c) An eastern sector, which extends from Panarea and Stromboli Islands to the Alcione and Palinuro seamounts. In this sector, volcanism started at about 0.8 Ma, and it is still active at Stromboli. Fumarolic activity characterizes the submarine zones around Panarea (Gabbianelli et al., 1990; Italiano e Nuccio, 1991; Calanchi et al., 1995a), and a very shallow seismicity characterizes all the eastern seamounts. A prevailing NNE-SSW to NE-SW striking fault system affects the Stromboli and Panarea Islands (Gabbianelli et al., 1993). This is also the strike of the Stromboli canyon, a morphological incision located between the Gioia basin and the Panarea and Stromboli volcanic complexes, which has been interpreted as the surface expression of NE-SW striking faults (Volpi et al., 1997).

Petrological data indicate that the evolution of the Aeolian volcanism is characterized by a two-stage activity (Beccaluva et al., 1985). During the older stage, products ranging from calcalkaline and high-K calcalkaline basalts to dacites were erupted, whereas during the younger stage, which started about 40 ka ago, shoshonitic and some undersaturated leucite-bearing lavas were emitted. These K-rich magmas are associated both in space and time to rhyolites and, in a lesser amount, trachytes (Crisci et al., 1991). Rhyolites were emitted at Panarea, Vulcano, Salina, and Lipari, and were generally erupted together with less abundant high-K calcalkaline basalts, andesites, dacites, and shoshonites. Mixing and mingling phenomena among these magmas are a common feature of the younger Salina, Lipari, and Vulcano

eruptions (De Rosa and Sheridan, 1983; Calanchi et al., 1993; De Rosa et al., 1996; De Rosa et al., 2003a). With the appearance of rhyolites, the energy of the eruptions also increased: volumes in the order of 0.5-1 km<sup>3</sup> were emitted during single explosive episodes [e.g. the Pollara eruptions, 24 and 13 ka (Calanchi et al., 1993); Mt.Guardia, 22 ka (Sheridan et al., 1987; De Rosa et al., 2003b)]. When not associated with less evolved magmas, the rhyolites were emitted as lava flows, domes (e.g. obsidians at Lipari and Vulcano; Panarea extrusions) or low-energy strombolian pyroclastics (e.g. Mt.Pilato pumice-cone at Lipari). Recent geochemical and isotopic studies highlighted strong differences in terms of incompatible trace element ratios and isotopic signatures, between the western-central and the eastern Aeolian arc (Fig.3).

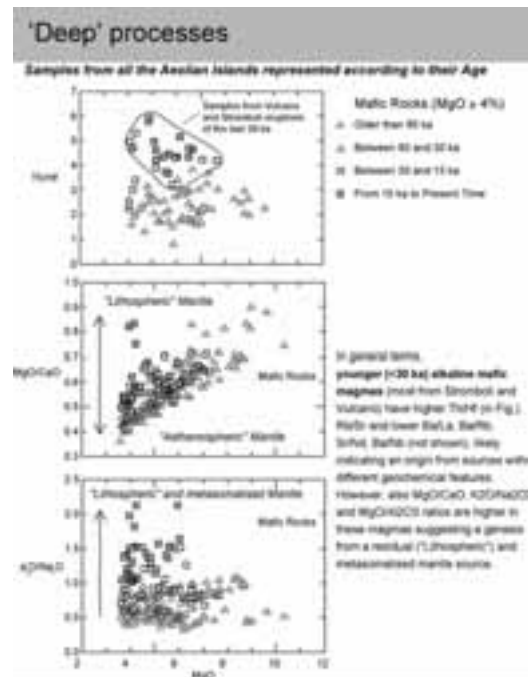


Figure 3 -  $K_2O/Na_2O$  and  $Th/Hf$  vs.  $MgO$  variation diagrams for Aeolian mafic rocks ( $MgO > 4wt\%$ ). From De Astis et al., 2003.

Rocks from the western-central islands (Alicudi, Filicudi, Salina, Lipari, Vulcano), have typical magmatic arc geochemical signatures, and relatively unradiogenic Sr-isotope compositions (Esperanca et al., 1992; Francalanci et al., 1993; De Astis et al., 2000, 2003; Gertisser and Keller, 2000). By contrast, the eastern sector (Panarea, Stromboli) has a more radiogenic Sr-isotope signature, and shows

trace element abundances intermediate between arc and intraplate compositions, even if some Panarea rocks show compositions partly similar to those of the mafic rocks from Alicudi and Filicudi, and partly intermediate between the compositions observed in the two sectors of the arc (Peccerillo, 2001; Calanchi et al., 2002a).

In conclusion, available geochemical, isotopic, and field data (e.g. Barker, 1987; Ellam and Harmon, 1992; Esperanca et al., 1992; De Astis et al., 1997), suggest that interaction between magma and upper crust is a significant evolutionary process in the Aeolian arc. However, geochemical and isotopic studies on mafic magmas, and on the crystalline basement, suggest that the main compositional differences between primary magmas are likely to have been inherited from a heterogeneous mantle source (De Astis et al., 2000, and references therein). The reasons for mantle heterogeneity are still a matter of discussion, although the majority of authors have suggested that it results from the interaction between various reservoirs, including MORB- and OIB-type mantle, and slab-derived sediments and fluids (e.g. Francalanci et al., 1993; De Astis et al., 2000, 2003; Calanchi et al., 2002a). In a recent paper, De Astis et al. (2003) in the light of structural, seismological and geochemical data, suggest that the rapid transition from CA and HKCA, to SHO and KS, products may reflect the transition from a collisional-type volcanism (CA), to post-collisional/rifting volcanism (SHO-KS).

Therefore the late phase of the Aeolian volcanism may be mainly related to the rifting-type processes, more than to the subduction processes. In this framework, the Aeolian volcanism might be related to post-collisional extension processes in an arc collision zone.

## Field Itinerary

### DAY 1

#### Stromboli

Stromboli stratovolcano, the northernmost island of the Aeolian volcanic arc, rises from a depth of about 2,000 m b.s.l., to an elevation of 924 m a.s.l. (Fig. 4), lying up on a 20 km thick continental crust.

The oldest subaerial rocks of the volcano, with an age of  $204 \pm 25$  ka (Gillot and Keller, 1993), is the Strombolicchio neck, located about 1.7 km NE of Stromboli, and belonging to the same submarine

edifice. The subaerial part of the main cone was built up during the last 100 ka, through mainly effusive activity and minor explosive eruptions. Six main periods of activity characterized the volcanological history of Stromboli (namely, from the oldest to the youngest: Paleostromboli I, II, III, Vancori, Neostromboli, Recent Period) (Hornig-Kjarsgaard et al., 1993; Pasquarè et al., 1993); and they were recognized on the bases of structural changes and stratigraphic unconformities. Several collapses of

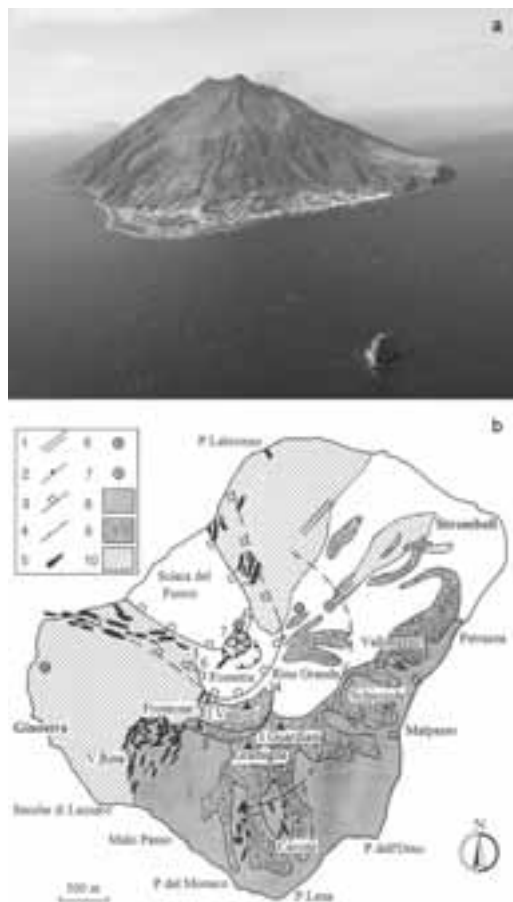


**Figure 4 - a) Panoramic view from the NE of Stromboli Island; b) Simplified geological map of the island, showing dikes and volcano-tectonic features. 1 = eruptive fissure; 2 = crater rim; 3 = flank and sector collapses; 4 = summit caldera; 5 = dike; 6 = young parasitic vent; 7 = active vent; 8 = Paleostromboli I, II and III lavas, and pyroclastic rocks; 9 = Vancori lava sequence; 10 = Neostromboli lavas and scoriae; the Recent and present day lavas and pyroclastic rocks are indicated in white. Numbers on the map refer to the different collapses. From Pasquarè et al. (1993).**



Figure 5 - Shaded relief map of the submerged extension of Sciara del Fuoco, with main morphological features described in the text. 1 = lateral walls of Sciara scar; 2 = identified limit of the fan-shaped deposits; 3 = levee; 4 = mounded features; 5 = slumped areas; Cy = canyon. From Romagnoli et al. (1993).

different natures (crater, caldera, flank, and sector collapses), alternated with periods of volcano building (Fig. 4). They were mainly crater and caldera collapses before 13 ky ago (up to and including the Vancori period), and mainly flank and sector collapses later on. In particular, after the Vancori period, four collapses affected the NW part of the cone, leading to the formation of some peculiar features, such as the Sciara del Fuoco scar, a steep trough on the NW flank of Stromboli (Fig. 5), and the crater terrace, where the present day activity takes place (Rosi, 1980; Pasquarè et al., 1993; Tibaldi, 2001).

The rock composition is typical of an orogenic setting, and displays large variations, from calc-alkaline (mainly basaltic-andesites), to potassic-alkaline (potassic trachybasalts and shoshonites); through high-K calc-alkaline (high-K basalts to high-K andesites), and shoshonitic (shoshonitic basalts to a few trachytes) (Fig. 6) (Francalanci et al., 1989; 1993; Hornig-Kjarsgaard et al., 1993). Strombolicchio lavas are calc-alkaline, as Paleostromboli II rocks, which are mainly constituted by lava flows. During Paleostromboli I and III, pyroclastic deposits (flow,

surge, and fall) and lavas, with mainly high-K calc-alkaline composition, were erupted. The Vancori period was mostly characterized by effusive activity, which erupted shoshonitic lavas, forming the highest peak and the youngest outcrops in the S and SE parts of the volcano. Neostromboli rocks are thin scoriaceous lava flows, with potassic-alkaline composition, which mainly form the NW part of the volcano, except for the Sciara del Fuoco scar (Francalanci et al., 1989, 1993; Hornig-Kjarsgaard et al., 1993). The rocks of the Recent period, younger than  $5.6 \pm 3.3$  ka (Gillot and Keller, 1993), are formed by, firstly, the pyroclastic cone of Pizzo Sopra la Fossa, with shoshonitic basalt composition, secondly, by the high-K basalts of S. Bartolo lavas, and, thirdly, by the products of the present day activity, which are younger than Pizzo pyroclastic rocks (Hornig-

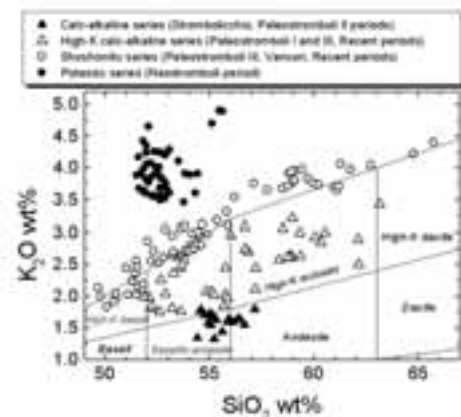


Figure 6 -  $K_2O$  versus  $SiO_2$  classification diagram for all the Stromboli rocks. Data are reported on water-free bases. Redrawn from Francalanci et al. (1993).

Kjarsgaard et al., 1993).

Rocks mainly have holocrystalline porphyritic seriate textures, with phenocryst contents ranging from about 10 to 55 vol.%. Plagioclase and clinopyroxene are the prevailing mineral phases. Olivine is present as phenocryst in the mafic rocks, up to basic andesites. Biotite and hornblende appear in the most evolved products of the shoshonitic and high-K calc-alkaline series, respectively. Orthopyroxene is mainly found in latites and basaltic-andesites (Fig. 7). Apatite and opaques are present as accessory mineral phases.

The potassium content of rocks is positively correlated with the incompatible trace element contents, but a near opposite correlation exists for the compatible



at the surface of the magma column, resulting in the formation of a jet of hot gas, and incandescent lava fragments. The explosions last for a few seconds, and take place at regular intervals, the most common time interval being 10-20 min. Explosive activity is associated with the continuous streaming of gas, with an estimated output of 6,000-12,000 t/day and consisting mainly of H<sub>2</sub>O (3200-6300 t/day), CO<sub>2</sub> (2900-5800 t/day), SO<sub>2</sub> (400-800 t/day), and minor HCl and HF (Allard et al. 1994). The routine activity of the volcano is periodically interrupted by lava flows within the Sciara del Fuoco, and by more violent explosions. Mid-scale explosions consist of short-lived blasts that eject meter-sized spatter, and blocks within a distance of several hundreds of meters from the craters. On average, two or three explosions per year has occurred over the past 100 years (Bertagnini et al. 1999). Less frequently, much more violent explosions occur. They produce showers of blocks, and incandescent fragments within a distance of kilometers from the craters, and often affecting the two villages on the coast.}

Black scoriae, scoriaceous bombs and lapilli, and lava flows are formed by a volatile-poor, Highly Porphyritic magma (hereafter "HP magma"). Two types of magmas are, instead, erupted from major explosions and paroxysms. The most voluminous juvenile component is an HP magma, which is erupted together with a highly vesiculated light pumice, representing a volatile-rich, Low Porphyritic magma (hereafter "LP magma") (Bonaccorso et al., 1996; Francalanci et al., 1999, 2003; Bertagnini et al., 1999; Métrich et al., 2001). Black scoriae and light pumice are often intermingled in the same ejecta. This persistent Strombolian activity began between III and VII century A.D. and it seems to be associated with the presence of two types of magma (Rosi et al., 2000).

The chemical and petrographic characteristics of rocks erupted since the beginning of the Strombolian activity have remained nearly constant.

Black scoriae and lavas have a highly porphyritic seriate texture (ca. 45-60 vol% of phenocrysts and microphenocrysts). Plagioclase is the most abundant mineral phase ( $\approx$  35 vol%), followed by clinopyroxene ( $\approx$  15 vol%), and olivine ( $\approx$  5 vol%). The anorthite (An) content of plagioclase generally ranges from 60% to 87%, the zoning is complex but normal in the rims. The largest phenocryst phase is clinopyroxene (up to 1 cm long), with a prevalent augite composition, but usually showing internal bands of diopside. Olivine is the second largest mineral phase in size, generally ranging from 64%

to 74% of Forsterite (Fo) content. Light pumice has poorly porphyritic seriate textures ( $<$  10 vol %), with glassy groundmass. Minerals consist of olivine, clinopyroxene and plagioclase, with variable proportions in the different samples. Fo content of olivine is from 68% to 86%, but the composition in equilibrium with the groundmass is around 81-86%. Phenocryst zoning is sometimes large and reverse. Clinopyroxene shows the same compositional range as clinopyroxene in scoriae and lavas, but zoning is usually reverse. An content of plagioclase ranges from 60% to 90%, with equilibrium crystals having An  $>$  80%. (Francalanci et al., 2003).

Scoriae, lavas and pumice compositions range from high-K to shoshonitic basalts (Francalanci et al., 1999, 2003; Rosi et al., 2000; Métrich et al., 2001). Pumice samples are slightly less evolved than scoriae and lavas (Fig. 9), whereas the glassy groundmasses of pumice are sharply distinct in composition from those of scoriae and lavas: pumice glasses are still shoshonitic basalts, but scoriae and lava glasses are shoshonites, with K<sub>2</sub>O between 3.5-5.2 wt%. This is evident for most of the major and trace elements (e.g. Fig. 10). Sr isotope ratios of scoriae and lavas from the beginning of the 20<sup>th</sup> century to around 1980-85 A.D., are constant, with an average of 0.70626, then start smoothly to decrease, up to the value of 0.70615 of present day scoriae. Pumice samples have significantly lower Sr isotope ratios than scoriae, with  $^{87}\text{Sr}/^{86}\text{Sr} \approx$  0.70610 (Francalanci et al., 1999). Nd isotope ratios of scoriae, lavas, and pumice from the major eruptions in 1996 and 1998 A.D., are nearly the same (around 0.51256) (Francalanci et al., 2003).

The general steady state conditions of the present plumbing system of Stromboli have been hypothesized on the bases of thermal and gas budget balances, and of the homogeneous composition of rocks erupted from the Strombolian activity (Giberti et al., 1992; Allard et al., 1994, 2000; Harris and Stevenson, 1997; Francalanci et al., 1999; 2003; Rosi et al., 2000). It has been also suggested that the HP magma resides and evolves in a continuously erupting, crystallizing and replenished shallow reservoir, where the steady state conditions are maintained. The LP magma, erupted as light pumice, represents the replenishing magma, which arrives from a deeper reservoir, and it is characterized by different physico-chemical conditions to that of the HP magma. The pre-eruptive process of evolution affecting the magmas which feed the present day activity of Stromboli can, therefore, be deduced as mixing, associated with fractional crystallization (Francalanci et al., 1999, 2003; Métrich et al., 2001).

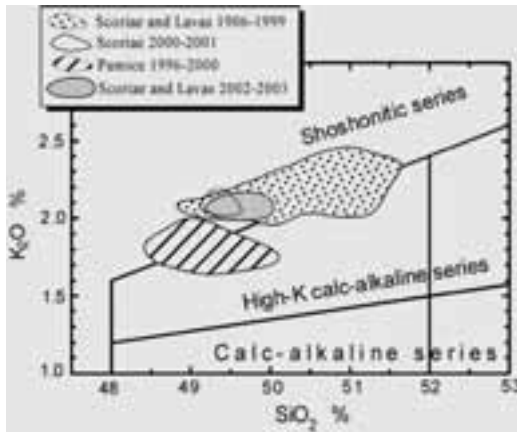


Figure 9 -  $K_2O$  versus  $SiO_2$  classification diagram showing the compositional fields for the rocks of the present day activity of Stromboli, including the scoriae and lavas from the 2002-2003 eruptive crisis. Data are reported on water-free bases. Data unpublished and from Francalanci et al. (2003.) with references therein.

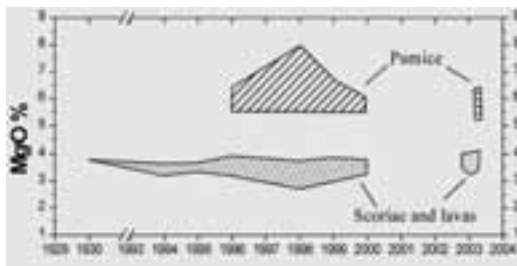


Figure 10 - Variation of  $MgO$  contents over time, for the glassy groundmasses of the scoriae, lavas, and pumice erupted by the present day activity of Stromboli, including the 2002-2003 eruptive crisis. Data unpublished and from Francalanci et al. (2003).

### 2002-2003 eruptive crisis

During the first seven months of 2003, Stromboli produced the most intense and dangerous eruptive crisis of the past three centuries. Due to the threat of (and eventual) slope failure and tsunamis, part of the resident population voluntarily left the island using air transportation facilities made available by the national Civil Protection authorities. The eruptive crisis started on 28 December 2002, and ended on 21 July 2003, when the volcano returned to its normal state of persistent activity. The volcanic crisis consisted in the combination of the following eruptive phases (Bonaccorso et al., 2003): i) the onset of the eruption, and the Sciara del Fuoco slope failure, ii) effusive eruption, and iii) the paroxysm explosion of 5 April, 2003. The volcanic hazard climaxed on December 30,

2002, and April 5, 2003, when a large tsunami wave hit the village of Stromboli and blocks fell on Ginostra.

### Onset of the activity and Sciara del Fuoco slope failure

The volcanic crisis started on December 28, 2002, when voluminous, unusually fast-moving lava flows were issued from several vents in the NNE sector of the Sciara del Fuoco. Lava flows reached the sea in various places, giving rise to moderate explosions and vapor emission. Between 28 and 30 December the lava flow activity was accompanied by significant displacement seawards of masses of volcanic materials, thus forming the infill of the Sciara del Fuoco, and by the formation of moderate volume debris avalanches. At 1:15 p.m. of 30 December 2002, slope perturbation, caused by eruptive phenomena, culminated in the catastrophic failure of the northern sector of the Sciara slope. Surveys conducted in January 2003 revealed that the collapse involved an elongated, irregularly-shaped, rock body with a maximum thickness of about 40 meters, which detached from both the subaerial and submarine portion of the Sciara, between 600 m a.s.l. and 600 m b.s.l. The catastrophic failure resulted in a strong sea level perturbation, and the concurrent generation of tsunami waves, which hit the village of Stromboli causing substantial damage, and a few injuries. The maximum height of the tsunami waves which hit the village, was about 9 m. The opening of an effusive vent at an elevation of 500 m caused the drop of the magma level in the volcano conduit, the collapse of the summit craters, and immediate cessation of the Strombolian activity.

### Effusive eruption

From 30 December 2002, to 14 February 2003, the volcano produced continuous lava emissions from a vent located at about 500m a.s.l. By mid-February, the effusive vent moved eastwards at about 550 m a.s.l. From mid February to 21 July, the effusive vent remained more or less stable, and the effusion rate progressively declined. By the end of the effusive eruption, the scar produced on the 30 December had been partially filled up, and a new lava bulge had been formed in the eastern sector of the Sciara, as a result of lava accumulation. Preliminary estimates indicate that the total volume of the erupted lava was in the order of 10 million of  $m^3$ .

### Paroxysmal explosion of April 5, 2003

In the first half of April, three explosions occurred in the summit craters on the 3<sup>th</sup>, 5<sup>th</sup> and 10<sup>th</sup> of this

month. The explosion which occurred on April 5th at 9:12 a.m. local time, was sudden and by far the most violent. The explosion consisted of a vertical jet of blocks and incandescent fragments, which generated a dark, 2 km high, convective column (Calvari, 2003). This column was blown south by the wind, producing the fallout of pumice in the sea between Stromboli and Basiluzzo. Meter-sized blocks launched several hundreds of meters above the vent fell back on the NE and SW flank of the volcano, up to a distance of 1.5-2 Km from the crater area. In the village of Ginostra, on the SW side of the island, a house and a rain-water tank were severely damaged by meter-sized falling blocks. In the same village, some houses reported broken windows due to the transit of a shock wave. The explosion deposited a familiar blanket of blocks and pumiceous bombs in the upper part of the mountain.

Scoriae and lavas erupted during the 2002-2003 eruptive crisis are highly porphyritic rocks, not different from those of the previous Strombolian activity, with phenocrysts of prevalent and smaller plagioclase, large clinopyroxene, and olivine. Even pumice from 5<sup>th</sup> April 2003 does not show any important petrographic changes in relation to the previously erupted pumice. The main mineral composition seems, however, to reveal some small differences from that of the older mineral phases.

Whole rock data of major and trace elements for scoriae and lavas (data up to January 2003) plot in the same compositional fields as previously erupted and less evolved scoriae and lavas (Figs. 9, 11). Even the compositions of glassy groundmasses (including the scoriae and pumice of the 5<sup>th</sup> April paroxysm) do not change significantly (Fig. 10). Sr isotope ratios in whole rocks, and groundmasses of scoriae, lavas and blocks (from paroxysm), range between 0.70614 to 0.70616, showing some fluctuations before and after the lava flow eruption. Pumice groundmass analysis reveals Sr isotope ratios of about 0.70611, similar to the previously erupted pumice.

**Sciara del Fuoco instability**

The morphostructural evolution of Stromboli has been dominated by caldera collapses and the gravitational failure of its flanks. Caldera structures have been inferred for the period older than 13 ka. Since then, Stromboli has produced at least four major collapses of the northwest flank of the cone. The older one, which affected the Vancori edifice, had an estimated volume of 2-3 km<sup>3</sup>. The following collapse episode (volume 1-1.5 km<sup>3</sup>), beheaded a 900 m high cone,

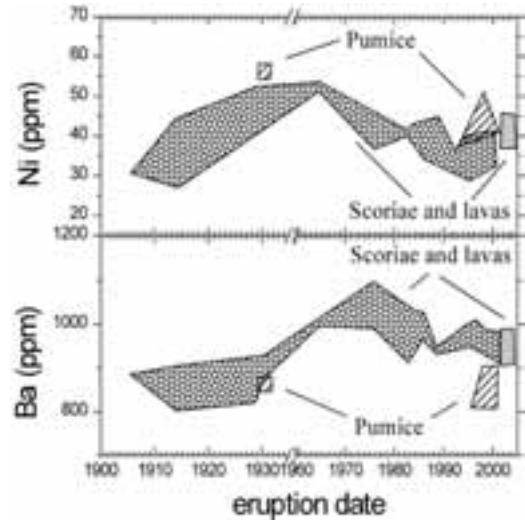


Figure 11 - Composition of scoriae and lavas from the eruptive crisis of 2002-200,3 and comparison with the variation of Ba and Ni contents over time for the rocks of the present day activity of Stromboli. Data unpublished, and from Francalanci et al. (2003) with references therein.

whose summit was situated above the present crater area. After this event, an about 1000 m high cone was formed (Pizzo Sopra la Fossa). The Pizzo Sopra la Fossa edifice was in turn largely dismantled by another gravitational failure (The Sciara del Fuoco collapse), during which volumes of about 1.08 km<sup>3</sup> of volcanic material slid into the sea. The last one generated the present depression of the Sciara. Material presently accumulated within the subaerial part of the Sciara del Fuoco, consists of loose debris with subordinate intercalations of lava flows. Below sea level, material is entirely made up of volcanic debris supplied by fast abrasion which was produced by sea wave action. The subaerial and subaqueous slope of the Sciara is 40-45°, very close to the angle of repose of the materials, and as a result, the slope is unstable and exposed to gravitational collapse that, in turn, can produce sea perturbations.

**Stop 1.1:**

In the locality of “La Petrazza”, in the NE flank of the island (close to the Stromboli harbour), the sequence of pyroclastic deposits and lavas of the *Scari complex* (Paleostromboli III), is well exposed. It overlies the Upper Paleostromboli I high-K basaltic-andesite lavas, which were erupted by a local eruptive center. The *Scari complex* is restricted to this part of the



**Stop 1.3:**

At about 300 m a.s.l., the path opens for the first time on the impressive view of Sciara del Fuoco, the deep scar formed in the present shape by the last lateral collapse of the NW part of the cone (Fig. 5). The sequence of Neostromboli lavas and associated aa scoriae is visible below, exposed by the collapse along the sides of the Sciara del Fuoco, and cut by several dykes (Fig. 4). The deposits of Sciara del Fuoco, representing the products of present day Strombolian activity (scoriaceous bombs and lapilli, blocks, lavas and ash), can be also observed from afar. The 2002-2003 lava flow, widespread all over the northern part of Sciara del Fuoco, is particularly evident.

Continuing towards the top, above the Neostrombolilavas, several outcrops of the Lazzaro pyroclastic deposits are found. They are mainly constituted of ash beds rich in accretionary lapilli, and testify to the occurrence of highly explosive activity at the end of the Neostromboli period.

Scoriae and pumice erupted during the more recent major eruptions and paroxysms (e.g. 1930 eruption?), are also visible around the path from about 400 m a.s.l. Large blocks erupted by the paroxysm of 5<sup>th</sup> April 2003 start to be found from about 500 m a.s.l. The Strombolian activity from the NE crater can be well observed from about 750 m. a.s.l..

Just before the Liscione peak (865 m. a.s.l.), the path leaves the Neostromboli rocks, and passes through a narrow ridge on the Upper Vancori lavas (biotite-bearing latites and trachytes) and breccias, which are in discordance with the deposits of the Recent period, which dip towards the Sciara del Fuoco depression.

The view down towards Stromboli village, allows us to have a look to the eruptive fissure of Vallonazzo (Neostromboli), and to the site of the other lateral vents present in the NE sector of the volcano.

**Stop 1.4:**

The top of Pizzo Sopra la Fossa (918 m a.s.l.) is the end of the ascent. Being 150 m above the active vents, it is possible (with good weather conditions), to have an impressive view of all the craters, and of the intermittent moderate Strombolian explosions. On average, there are about three craters with about five eruptive vents continuously degassing. Typical strombolian explosions take place from the vents of the NE crater, which is usually the most active, and

from the SW crater. The morphology and dynamics in the crater terrace, however, is subjected to change over time.

We will wait here until dusk. Indeed, only in the dark, it is possible to estimate the real size and shape of the different magma fountains.

During the daytime, we can have a look at the Pizzo Sopra la Fossa yellow tuffs, which are composed of discordant pyroclastic falls and flows, with a basaltic shoshonitic juvenile composition.

It is also possible to observe the Vancori sequence of lavas and a few pyroclastic rocks, forming the close and highest peak (924 m a.s.l.) of the volcano, cut by the first huge lateral collapse towards the NW (at about 13 ky) (Fig. 4). The rims of this, and of the younger lateral collapses, are also visible all around, as are several geologic discordances.

Scoriaceous bombs, blocks, and pumice from the recent major eruptions can be seen towards the "Fossetta" valley, whereas single, well-preserved, clinopyroxene crystals (augite) can be collected from the lapilli and coarse ash emplaced by the normal activity eruptions.

**DAY 2**

The second day will be devoted to illustrating the stratigraphical evolution of the island of Lipari, with special attention paid to the complex relationships between volcanic activity and Late Quaternary eustatic fluctuations. In order to have the best conditions of sun exposure, we propose a counterclockwise tour of the island; as a consequence, the description of the stratigraphical succession will be strongly conditioned



Figure 13 - Bathymetric sketch map of the Aeolian Arc (southern Tyrrhenian Sea)

by the succession of outcrops encountered along the tour. The stratigraphy is defined by taking into account the relationships between volcanic products and ancient marine deposits of Tyrrhenian age: therefore, the volcanic succession will be described in terms of pre-Tyrrhenian, Tyrrhenian and post-Tyrrhenian age units.

### Lipari

The Island of Lipari represents the emerged portion of a broad volcanic edifice that rises about 2000 m from the sea floor in the central sector of the Aeolian Arc, in the southern Tyrrhenian Sea (Fig. 13).

The age of volcanic activity on Lipari ranges from at least 223 ka to the present time. This age span takes into account dates derived by K/Ar (Cortese *et al.*, 1986; Gillot, 1987; Crisci *et al.*, 1991), Ar/Ar (Lucchi, 2000a) and  $^{14}\text{C}$  techniques (Crisci *et al.*, 1983; Losito, 1989).

Indicators of three raised fossil shorelines (Fig. 14), located at elevations of 43-45 metres asl (I order), 23-27 m (II order), and about 12 m (III order), are recognized on the Island of Lipari (Calanchi *et al.*, 2002b; Lucchi *et al.*, 2003).

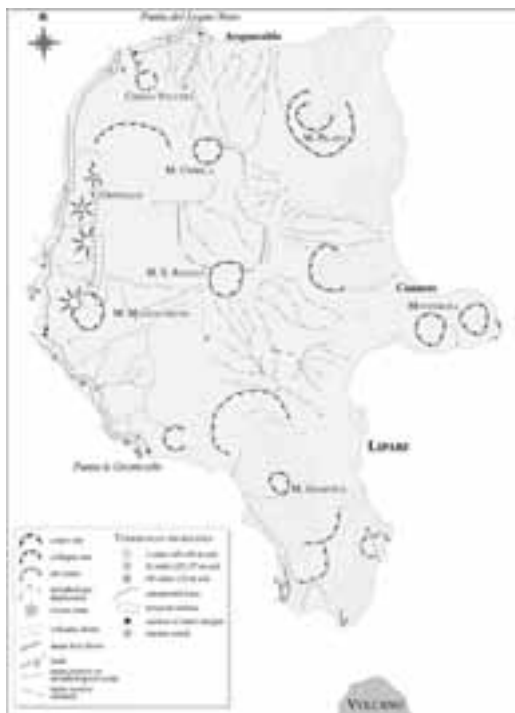


Figure 14 - Geomorphological and volcano-tectonic sketch map of Lipari, and distribution of the Tyrrhenian fossil shorelines (from Tranne *et al.*, 2002; modified).

Detailed evaluation of stratigraphic relationships to the volcanic substratum, allows for their correlation with Late-Quaternary eustatic highstands of Tyrrhenian age, corresponding to marine oxygen isotope substages (MIS) 5e, 5c, and 5a, dated to 124, 100, and 81 ka, respectively.

The alternation of marine deposits with volcanics allows for main unconformities to be defined in the stratigraphy of Lipari, and these represent significant hiatuses of volcanic activity. The unconformities have been produced by marine erosional episodes which corresponded to the discrete eustatic highstands, and following subaerial erosion. The hierarchy of the unconformities is established by taking into account the potential extensibility at a regional scale. By taking this approach, two first order unconformities ( $U_I$  and  $U_{II}$ ), have been introduced (Tranne *et al.*, 2002), thus fixing the boundaries of the marine deposits of Tyrrhenian age (Figs. 15a,b and 16), which have been correlated on most of the Aeolian archipelago.  $U_I$  is the marine erosional surface related to the eustatic highstand, corresponding to MIS 5e, whereas  $U_{II}$  is the erosional surface produced by strong subaerial erosion processes, which are related to the sea level lowering at the end of MIS 5.

Although not synchronous, these unconformities developed over a short time span and, therefore, they assume an important chronostratigraphic significance, and allow main stages in the geological evolution of Lipari to be put in evidence (Fig. 15b). The building of the island has been described as the result of two mainly constructive stages of strong volcanic activity, pre-Tyrrhenian and post-Tyrrhenian, spaced out by the Tyrrhenian stage and characterized by the alternation of marine erosional episodes with volcanic activity (Figs. 15a,b, and 16).

The pre-Tyrrhenian stage ranges in age from ca. 220 ka to 124 ka (Fig. 14b), and consists of several episodes of strong volcanic activity, during which the products of the *Paleolipari* informal unit and Piano Grande Synthem (Fig. 15a, b) were emplaced.

- The *Paleolipari* informal unit includes the oldest outcropping products (scoriaceous deposits, lava flows, and subordinate hydromagmatic pyroclastics), CA basaltic-andesite in composition. They are related to the mainly strombolian and effusive volcanic activity of several eruptive centers located along the west coast (Timpone Carrubbo, Monte Mazzacarusu, Timpone Pataso, Timpone Ospedale, Valle di Pero, Pietrovito, and Chiesa Vecchia; Fig. 15, sections c-o) and, subordinately, in the central-

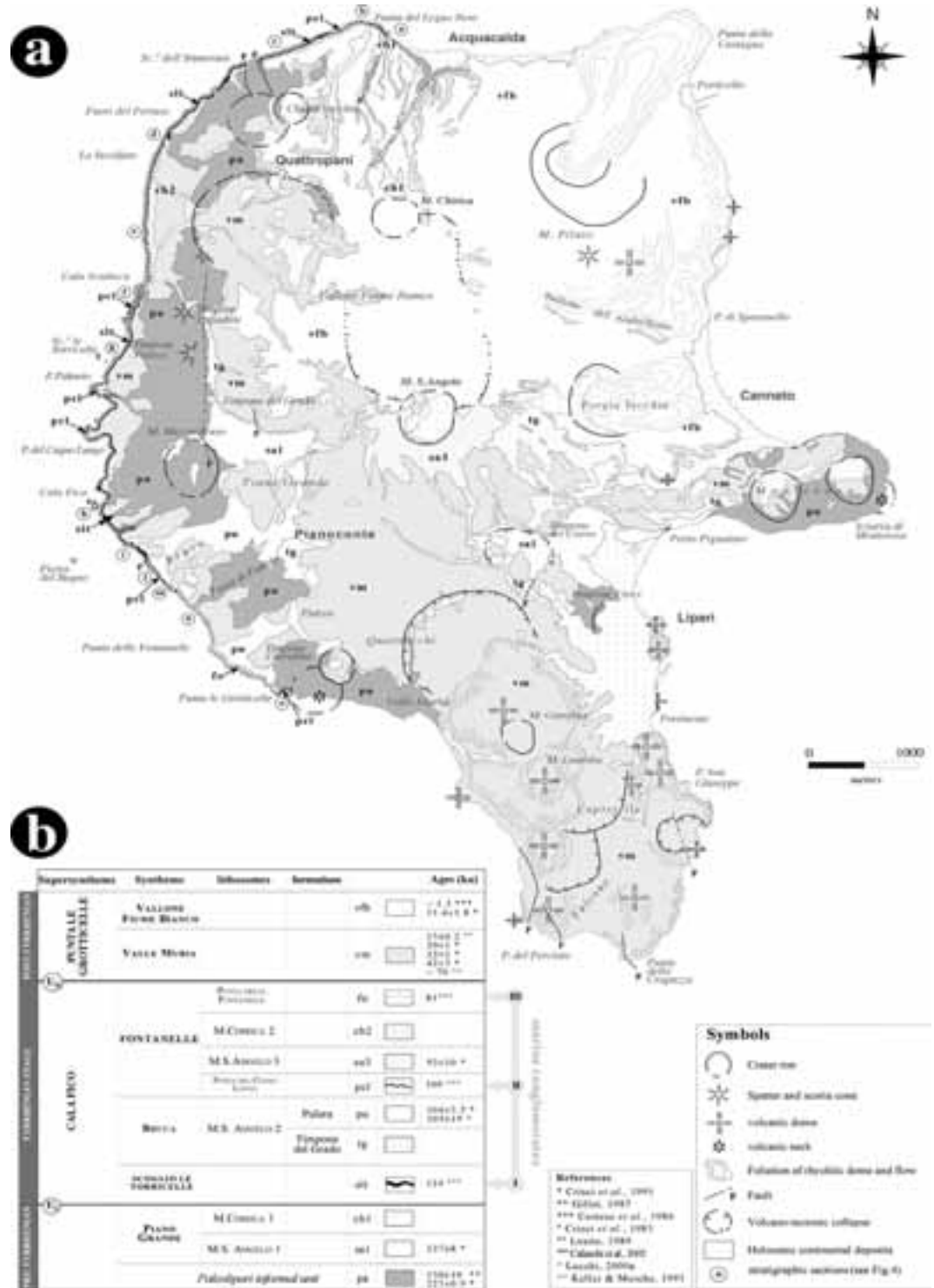


Figure 15 - Geological sketch map of Lipari (from Lucchi et al., 2003; modified).

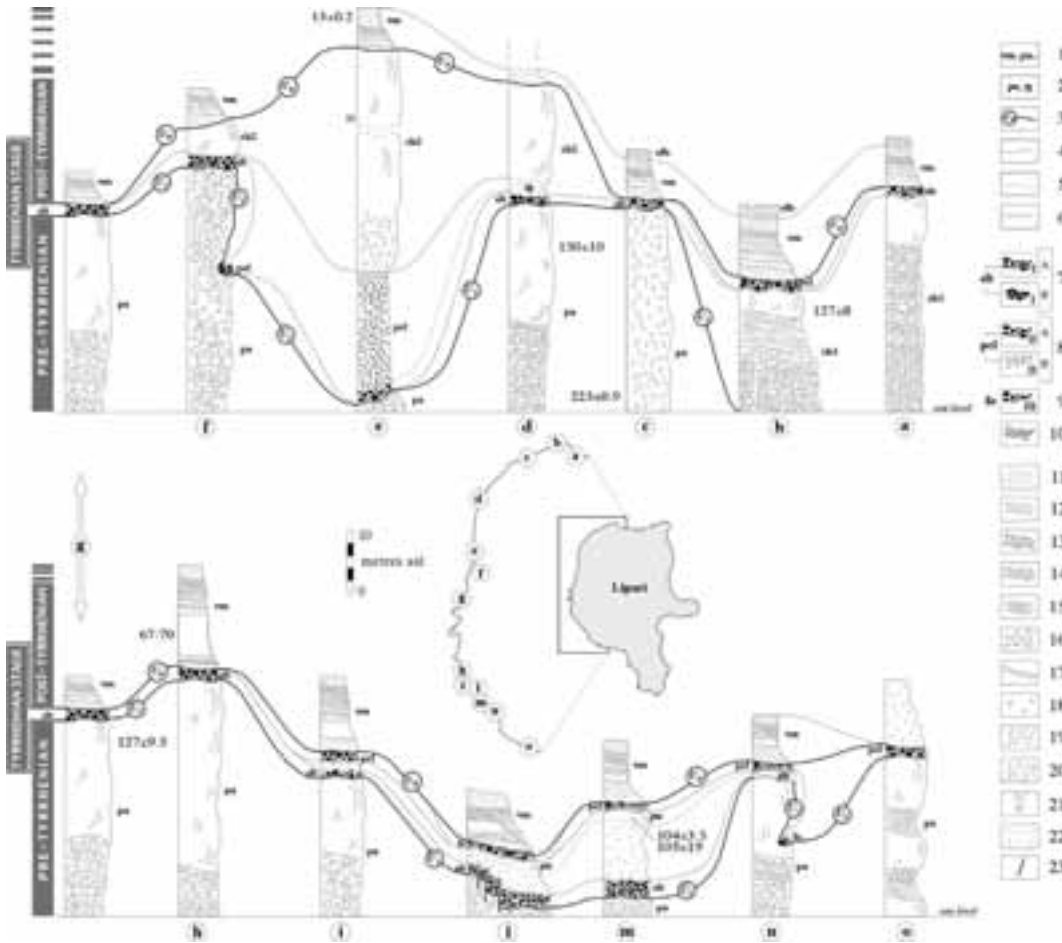


Fig. 16 - Correlation of stratigraphic sections along the west coast of Lipari (from Lucchi *et al.*, 2003; modified). Symbols: (1) main stratigraphic units (see Fig. 15); (2) “cordierite-bearing lavas” and “leaf-bearing pyroclastics” (Pulera and Timpone del Grado formations; see Fig. 15); (3) main stratigraphic correlations; (4) and (5) minor stratigraphic correlations; (6) paleosol; (7) I order fossil shoreline (st; see Fig. 15): A, littoral conglomerates; B, cemented littoral conglomerates; (8) II order fossil shoreline (pcl; see Fig. 15): A, littoral conglomerates; B, sands; (9) III order fossil shoreline (fo; see Fig. 15): littoral conglomerates; (10) “cordierite-bearing lava” pebbles; (11) lapilli tuffs and tuffs; (12) pumiceous pyroclastics; (13) loose scoriaceous lapilli; (14) welded scorias; (15) stratified pyroclastics; (16) clastogenic lavas; (17) exotic pyroclastic layers; (18) massive lava; (19) columnar-jointed lava; (20) brecciated lava or carapace; (21) dyke; (22) slope detritic deposit; (23) fault.

eastern sector of Lipari (Monterosa, Timpone Croci). Radiometric ages of  $223\pm 0.9$  ka (K/Ar date; Crisci *et al.*, 1991),  $150\pm 10$  and  $127\pm 9.5$  ka (K/Ar average dates; Gillot, 1987) have been obtained for these products.

- The Piano Grande Synthem comprises lavas and hydromagmatic pyroclastics (CA to HKCA basaltic-andesite, to andesite in composition) related to the first phase of volcanic activity of the NNW-SSE aligned Mt. S. Angelo and Mt. Chirica stratovolcanoes, located in the central

sector of Lipari. Lavas of the Mt. S. Angelo eruptive centre are dated to  $127\pm 8$  ka (K/Ar date, Crisci *et al.*, 1991).

The Tyrrhenian stage, ranging from 124 to 81 ka (Fig. 15b), was characterized by recurrent sea-level highstanding episodes, during which marine reworking processes occurred on the coastal slopes of the growing volcanic edifice, and caused the emplacement of marine conglomerates, sands, and terraces. This stage is also characterized by several episodes of volcanic activity, with the emplacement

of large volumes of lavas and pyroclastics related to the building of the Mt. S. Angelo and Mt. Chirica stratocones. The resulting interbedded marine and volcanic deposits are stratigraphically comprised in the Cala Fico Supersynthem, which is divided into the Scoglio Le Torricelle, Bruca, and Fontanelle Synthems (Fig. 15a,b).

- The Scoglio Le Torricelle Synthem includes the marine conglomerates (Fig. 16, sections a, c-d, f-m) related to the I order fossil shoreline (at an elevation of 43-45 m asl; Fig. 14) which is attributed to the Tyrrhenian eustatic highstand, corresponding to MIS 5e (124 ka). The conglomerates occur in the western coastal sector between P. del Legno Nero, and Vallone dei Lacci, with an average thickness of 2 m (up to 20-25 meters near Cala Sciabeca, where reworked conglomerates outcrop).
- The Bruca Synthem includes the volcanics which made up the main portion of the Mt. S. Angelo stratocone (Monte S. Angelo 2 lithosome; Fig. 15a, b): they consist of peculiar “leaf-bearing pyroclastics” (Timpone del Grado formation), and CA andesite lava flows (“cordierite-bearing lavas”), the latter ones dated to 104±3.5 ka and 105±19 ka (Pulera formation; Figs. 15b and 16 sections l-n).
- The Fontanelle Synthem comprises the volcanics related to the final building stages of the Mt. S. Angelo (Monte S. Angelo 3 lithosome, dated at 92±10 ka) and Mt. Chirica stratocones (Monte Chirica 2 lithosome). The volcanic products are interbedded with the raised marine conglomerates of II and III order (Punta del Cugno Lungo and Punta delle Fontanelle lithosomes, Fig. 15b), which are attributed to MIS 5c and 5a, dated to 100 ka and 81 ka, respectively.

During the post-Tyrrhenian stage, ranging in age from 81 ka to the present time, sea-level was, for most of the time, considerably lower than at present, so that marine erosion and deposition affected portions of the volcanic edifice which are now submerged. In particular, a well-developed marine platform, likely formed during the last glacial lowstand, has been recognized at an average depth of 105-120 m bsl (Chiocci and Romagnoli, in press). During this time span, most of the southern and north-eastern portions of the island of Lipari were built up, with the occurrence of several episodes of strong volcanic activity, and with the emplacement of pyroclastics of exotic provenance. These volcanics are included in the Punta Le Grotticelle Supersynthem, which

is divided into the Valle Muria and Vallone Fiume Bianco Synthems (Fig. 15b).

- The Valle Muria Synthem includes the products related to recurrent strong volcanic activity, and this activity is mainly focused in the southern sector of the island, and subordinately in eastern Lipari. These products consist of widespread pumiceous, hydromagmatic pyroclastics associated with four effusive phases characterized by the emplacement of NNW-SSE and N-S-aligned volcanic domes, HKCA rhyolite in composition. The first phase of effusion of domes is dated to 42±3 ka (K/Ar date; Crisci *et al.*, 1991) and 40.5±3.1 (K/Ar date; Gillot, 1987), whereas the second, the third, and the fourth ones were emplaced in the 37-23 ka, 22-20 ka, and 13-11 ka timespans (Tranne *et al.*, 2002, and references therein). The pumiceous hydromagmatic pyroclastics are emplaced during explosive phases, which precede the recurrent effusive phases of activity. These pyroclastics, in particular the ones of the “Monte Guardia sequence”, are widespread over the entire Island of Lipari, and are interbedded with tephra of exotic provenance. Among the exotic tephra, at least twelve layers of the well-known, widespread “Brown Tuffs” have been identified, together with tephra correlated to the “Grey Porri Tuffs” from the Island of Salina, the “Ischia Layer” and the “Lower Pollara Tuffs” from the Island of Salina (Tranne *et al.*, 2002, and references therein). The interbedded local and exotic pyroclastics form a peculiar pyroclastic succession which represents a significant stratigraphic marker: the succession was emplaced in the chronological interval between more than 70 ka, (the age of the “Grey Porri Tuffs” located at the bottom of the succession), and 13 ka, (the age of the “Brown Tuff” layer located at the top of the succession) (Tranne *et al.*, 2002, and references therein).
- The Vallone Fiume Bianco Synthem comprises pyroclastics and lavas, HKCA rhyolite in composition, which are related to the recurrent volcanic activity focused in the north-eastern sector of Lipari. The pumiceous pyroclastics are widespread, and were emplaced during explosive hydromagmatic phases, which preceded effusive phases, and these latter were characterized by the emplacement of viscous rhyolitic lava flows and flowing domes. Several phases of volcanic activity, ranging in age from 11.4±1.8 ka (K/Ar

date; Crisci *et al.*, 1991) to about 1.3 ka (Cortese *et al.*, 1986), occurred with regard to the eruptive centers of Vallone di Gabelotto, Monte Pilato, and Forgia Vecchia.

### Fossil shorelines

Raised fossil shorelines are recorded along most of the west coast (between Punta le Grotticelle and Punta del Legno Nero; Fig. 2), and only in a few places along the east coast (nearby Porto Pignataro and Monterosa) of Lipari (Calanchi *et al.*, 2002b). Along the west coast, fossil shorelines occur mainly on the steep coastal cliffs, and are indicated by sloping, terraced surfaces, whose present distribution is strongly conditioned both by the covering of more recent deposits, and by subaerial and submarine reworking processes. The most visible feature consists of marine platforms (capped by littoral conglomerates), whose inclined sections outcrop at different elevations (Fig. 17).



**Figure 17** - At Cala Fico, the I order terraced surface (mp = marine platform, at elevation of 30-40 m asl; co = littoral conglomerates of the Scoglio le Torricelle Synthem; see Figure. 15) cuts lavas and pyroclastics (A) which are related to the Paleolipari informal unit (M. Mazzacarusso eruptive centre). The surface is capped by the Valle Muria Synthem pyroclastic succession (B). (From Lucchi *et al.*, 2003; modified).

In places, transversal sections of the original terraced surfaces have been observed: there, particular attention has been devoted to the identification (and to the measurement of the elevation) of the inner terrace margins or of the marine notches (Fig. 18a, b), as these are considered as representing the shoreline at the time of a sea-level peak.

Marine deposits consist of cliff base conglomerates capping the marine platforms, of reworked conglomerate deposits lying on submarine erosional surfaces, and of submerged beach sands. A detailed lithological study of the conglomerates has provided relevant stratigraphical constraints: the presence of pebbles of "cordierite-bearing lava" (Pulera formation; Figs. 14b and 15, sections l-n) in the littoral conglomerate outcropping between Bruca and

Punta le Grotticelle (Fig. 18) allows us to estimate the maximal age for the corresponding marine platform (Lucchi, 2000a).

A flight of three fossil shorelines has been inferred from the evaluation of main morphological features, such as inner margins and notches, and of the cross-cutting relationships (Lucchi *et al.*, 1999; Calanchi *et al.*, 2002b; Lucchi *et al.*, 2003). The fossil shorelines occur (Figs. 13 and 15) at the present elevation of 43-45 m (I order), 23-27 m (II order), and ~12 m (III order). A continuous and complete threefold staircase did not form, or has not been preserved on the island, because the shorelines may be missing or laterally discontinuous, owing to subaerial reworking

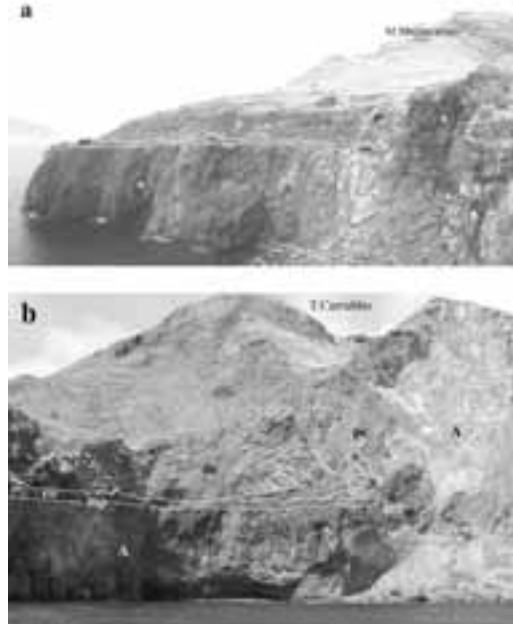


**Figure 18** - Emergent remnants of fossil shorelines (from Lucchi *et al.*, 2003; modified). (a) Terraced surface occurring on the steep coastal cliff at Cala Fico (im = inner margin, at elevation of ca. 45 metres asl; pc = palaeocliff; mp = marine platform; co = littoral conglomerates); this surface cuts massive lavas (A) related to the Paleolipari informal unit (Monte Mazzacarusso eruptive centre) and is extensively capped by the pyroclastic succession of the Valle Muria Synthem (B). (b) Terraced surface occurring on the steep coastal cliff at Punta le Grotticelle (im = inner margin, at elevation of 25-27 metres asl; pc = palaeocliff; mp = marine platform; co = littoral conglomerates); the surface cuts massive lavas (A) related to the Paleolipari informal unit (T. Carrubbo eruptive center) and is covered by ancient slope detrital deposits (de). (From Lucchi *et al.*, 2003; modified).



**Figure 19** - At Bruca, four normal faults (F) displace the remnants of a I order terraced surface ( $co_1$  = cemented conglomerates;  $mp_1$  = marine platform): the terraced surface cuts lavas (A) related to the Paleolipari informal unit. The lowered sector is filled with detrital deposits (det). II order ( $co_2$  = littoral conglomerates;  $mp_2$  = marine platform) and III order ( $co_3$  = littoral conglomerates;  $mp_3$  = marine platform) terraced surfaces overcut the detrital deposits and are not affected by the faults. Both surfaces stratigraphically lie on the "cordierite-bearing lavas" (B) because the  $co_2$  and  $co_3$  conglomerates contain pebbles of this peculiar lithotype. The stratigraphic succession is capped by the pyroclastics of the Valle Muria Synthem (C), and by recent detrital deposits (D), which partially hinder the stratigraphic contacts. (From Lucchi *et al.*, 2003; modified).

processes or to marine erosion during the formation of younger shorelines.

The fossil shorelines at Lipari are dated on the basis of their chronological intervals of formation, the cross-cutting relationships, and the inferred correlation with marine oxygen isotope stages (MIS). The chronological intervals of formation of the fossil shorelines are constrained by the stratigraphical relationships between volcanic products and marine deposits related to each shoreline (Fig. 4; Lucchi *et al.*, 2003). Moreover, the cross-cutting relationships between distinct shorelines are taken into account, assuming a similar trend of uplift (as usually assumed for Late Pleistocene marine terraces; Bordoni and Valensise, 1998). The conclusions reached are that the three shorelines are not older than the Last Interglacial. In particular, the I order shoreline could develop only between about 130 and 105 ka, whereas the II and III orders developed between about 105 and >70 ka. According to these stratigraphic constraints, the staircased shorelines can therefore be correlated, and indirectly dated, to the peaks of a global eustatic curve, e.g. the curve proposed by Chappell and Shackleton (1986), which has not been modified, for the period considered, by the revision suggested by Chappell *et al.* (1996). A clear correlation appears between the I order shoreline, and the eustatic peak

corresponding to MIS 5e, dated to 124 ka, which corresponds to the Eutyrrhenian in the Mediterranean Quaternary marine stratigraphy (Vai, 1996). The II and III order shorelines can be reliably attributed to the eustatic peaks which correspond to MIS 5c and 5a, dated 100 and 81 ka, respectively (Fig. 20).

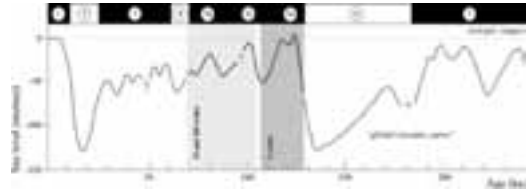


**Figure 20** - Correlation of the fossil shorelines of Lipari to the eustatic peaks and associated marine oxygen isotope stages, according to the curve of Chappell and Shackleton, 1986. The correlation takes into account the reconstructed intervals of formation (in grey). (From Lucchi *et al.*, 2003; modified).

Chronological and height data relative to the three orders of fossil shorelines have been used to estimate rates of vertical mobility occurring at Lipari in the last 125 ka (Lucchi *et al.*, 1999; Calanchi *et al.*, 2002b). In fact, a flight of raised fossil shorelines is the geologic record of Late-Quaternary sea-level fluctuations, superimposed on a rising coastline (Lajoie, 1986, and references therein). So, assuming that the formation of fossil shorelines corresponds with sea-level peaks, we can estimate the relative contribution of glacio-eustatic sea-level changes to their present elevation, thus obtaining the vertical displacement which affects each shoreline. This estimate is computed with a numeric and graphic approach (Fig. 21): by assuming a constant uplift between the time of formation of each shoreline and present time, and by plotting the displacement of each dated shoreline as a function of its age, we can estimate the relevant uplift rates. A continuous and regular mean uplift rate of ~0.34 mm/a results for the last 125 ka (Fig. 21): this rate is quite constant if we consider separately the values calculated for the I, II, and III order shorelines (0.31, 0.34, and 0.38 mm/a respectively).

Such a regular uplift trend is confirmed by the almost horizontal distribution of the shorelines in the shore-parallel profiles along the west coast of Lipari: this homogeneous height distribution is only locally offset by normal faults (Figs. 114 and 19). If, on the other side, partial uplift rates are estimated (i.e. from vertical displacement occurring between the formation of two shorelines), a constant mean uplift rate of ca. 0.16 mm/a is obtained for the time intervals

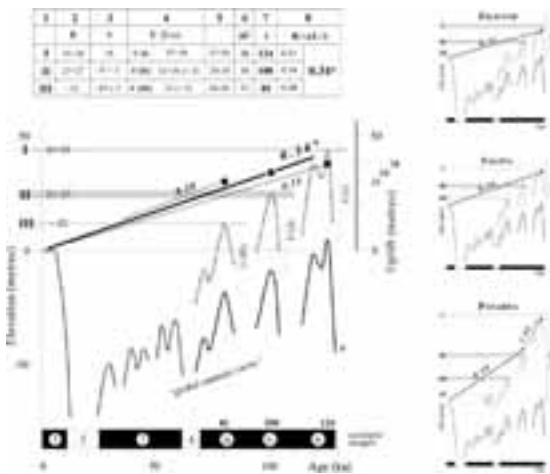


**Figure 21 - Numeric and graphic estimate of vertical movements of the volcanic edifice of Lipari during the last 125 ka. Models for the Islands of Filicudi, Salina and Panarea are also provided (Lucchi, 2000b). Legend: 1 = order of raised shorelines; 2 (E) = present elevation (metres asl) of the raised shorelines; 3 (e) = original elevation (m asl) of marine palaeo sea-level, corresponding to the formation of the raised shorelines (from the eustatic curve of Chappell and Shackleton, 1986); 4 (U) = uplift (in meters) of the raised shorelines (from column 4); 5 = ranges of uplift values, related to the fossil shorelines (from column 4); 6 (aU) = average uplift values (from column 5); 7 (t) = age (ka) of the raised shorelines; 8 (R) = mean uplift rate values in m/ka=mm/a (\*= mean of the values obtained). (From Lucchi *et al.*, 2003; modified).**

124-100 ka, and 100-81 ka (*Tyrrhenian* stage). This represents a further confirmation of the notably regular vertical behaviour of the volcanic edifice of Lipari. Evidence of rapid submergence during the last few centuries, opposite to the long-term uplift trend, has been observed only in some places on the east coast of Lipari (Calanchi *et al.*, 2002b). This process occur at rates considerably higher (ca. 10 mm/a) than the relative sea-level rise estimated for the coasts of Sicily in the same period (Antonioli *et al.*, 2002), and, for this reason, it is explained with the occurrence of prominent neo- or volcano-tectonics (Calanchi *et al.*, 2002b). Although such submergence movements are likely to be responsible for the independent motion of discrete sectors of the volcanic edifice of Lipari, the long-term pattern which is put in evidence by the coastal elevation changes, is one of persistent emergence (Calanchi *et al.*, 2002b). The average uplift rate estimated for the Island of Lipari (0.34 mm/a during the last 125 ka), is fully concordant with rates similarly estimated for Filicudi and Salina (0.31 and 0.36 mm/a, respectively; Lucchi, 2000a, b) for the same period (Fig. 20), but it differs from that

obtained for Panarea (variable, during the last 125 ka, between 0.69 and 1.56 mm/a; Lucchi *et al.*, 1999). These results indicate a similar trend of continuous uplift for the whole central part of the Aeolian Arc (Lucchi *et al.*, 2003). Crustal vertical movements of the volcanic edifices are interpreted as the result of interaction between punctuated eruptive, volcano- and neo-tectonic processes (transitory and active at local scale), and long-term sustained tectonic processes (slower, usually of lower magnitude and active at regional scale). In this view, the continuous and constant, long-term uplift trend occurring in the whole central-western Aeolian Arc during the Late-Quaternary should be explained by assuming a prevailing regional tectonic component. Regional crustal uplift at rates <1.21 mm/a (Bordoni and Valensise, 1998) is known to affect the whole inner sector of the Calabrian Arc, and has done so since the Mid-Pleistocene. Here, crustal deformations are connected with the subduction of the Ionian plate, the main geodynamic process which controls the geological evolution of the southern Tyrrhenian Sea (Amato and Montone, 1997; Gvirtzman and Nur, 1999). These results indicate that vertical movements, due to volcanic and volcano-tectonic processes, have not been intense enough to condition the vertical mobility of all the volcanic edifices. Volcano- and neo-tectonic processes have been brought up to explain the local occurrence of historical submergence trends (5-10 mm/a in the last centuries) evident in some places along the eastern coast of the Island of Lipari (Calanchi *et al.*, 2002b). On the other side, at Panarea (located in the eastern Aeolian arc), where vertical movements are continuous but not constant in time, eruptive and volcano-tectonic processes seem to play a significant role in controlling the long-term coastal tectonics (Lucchi *et al.*, 2003).

#### General conclusions

A threefold staircase of fossil shorelines, attributed to a *Tyrrhenian* age, has been defined along the emerged slopes of Lipari. They have been used as significant stratigraphic and morphotectonic markers.

From a stratigraphic point of view, marine deposits (and their boundaries) allow main unconformities in the geological evolution of Lipari to be defined. Two first order unconformities,  $U_I$  and  $U_{II}$ , have been introduced in the stratigraphy of Lipari, and then correlated at Panarea and Filicudi.  $U_I$  and  $U_{II}$  must represent significant stratigraphic constraints for the whole Aeolian archipelago. They allow main evolutionary stages to be uncovered. In particular, the





**Figure 24 - Shore-parallel vertical profile of the eastern sector of Monterosa, eastern Lipari, where a natural stratigraphic section of the Monterosa lithosome is visible. In the basal portion of the cliff, a cross section of the Sciarra di Monterosa tuff ring occurs: the tuff ring is made up of hydromagmatic (sc1a) and scoriaceous pyroclastics (sc1b), and is capped by massive lavas (sc2). In the middle portion, scorias and lavas of the Pignataro di Fuori formation (pf) lie on a well-developed subaerial erosion surface, which cuts the remnants of the Sciarra di Monterosa formation. The stratigraphic succession of the Monterosa lithosome, is closed by scoriaceous pyroclastics and lavas of the Monterosa formation (mo1 and mo2). At the top of the cliff, a thin layer of Brown Tuffs (pi=Pianoconte formation) occurs.**

### Stop 2.1:

*Locality:* Monterosa

*Description:* Pre-Tyrrhenian volcanics. Cross-section of the “Sciarra di Monterosa” tuff-ring, where the transition from hydromagmatic pyroclastics, to

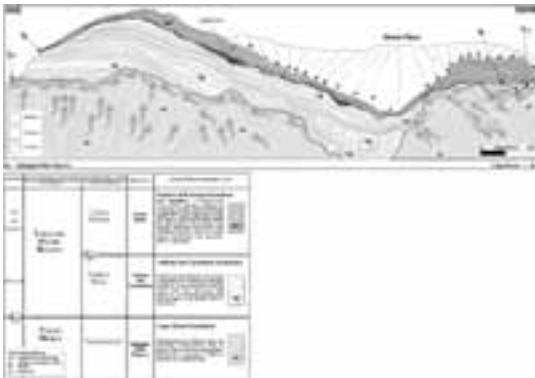


**Figure 25 - Shore-parallel vertical profile between Spiaggia della Papesca and Capo Rosso (eastern Lipari), where a natural stratigraphic section is shown. The rhyolitic endogenous dome of the Capo Rosso formation (cr), is capped by the pumiceous pyroclastics of the Vallone del Gabellotto (vg), and Sciarra dell’Arena formations (sa2). These stratigraphic relationships make evident the II order unconformity L4 and the III order unconformity lg. (From Lucchi et al., 2004).**

magmatic pyroclastics and lavas is exposed. The tuff-ring is covered by the “U Mazzuni2” scoria cone.

### Stop 2.2:

*Locality:* From Spiaggia della Papisca, to Punta delle Rocche Rosse.

*Description:* Post-Tyrrhenian volcanics (11-1.3 ka). We will describe the stratigraphical relationships between different superimposed orders of rhyolitic domes and related pyroclastics. The internal structures (foliation and rampart structures), of the famous Rocche Rosse obsidian lava flow will be observed.

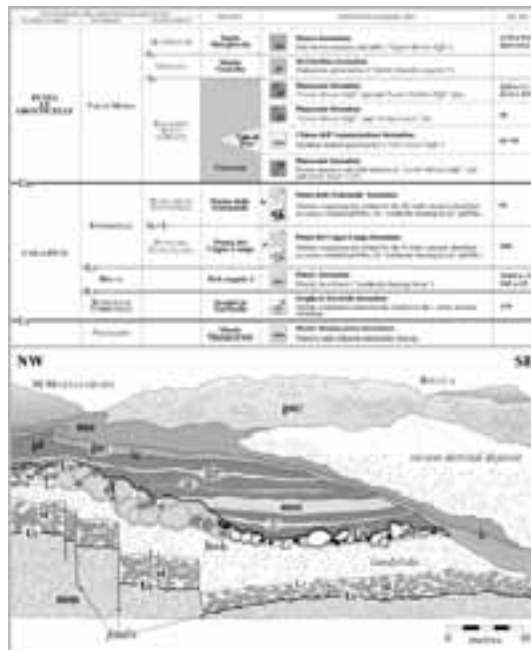


**Figure 26 - Shore-parallel vertical profile near Bruca (central western sector of the island), where a natural stratigraphic section is exposed: the cross-cutting relationships between the three orders of fossil shorelines and main unconformities are particularly visible.  $U_p, U_{n1}$  = I order unconformities; L2 - L3 = II order unconformities; lb - lb = III order unconformities. (From Tranne et al., 2002; modified).**

### Stop 2.3.:

*Locality:* From Punta del Legno Nero to Punta le Grotticelle.

*Description:* Pre-Tyrrhenian volcanics (<125 ka) and Tyrrhenian volcanics and marine deposits (125-81 ka). The pre-Tyrrhenian units show the typical features of strombolian and hawaiian eruptive

style. The Tyrrhenian deposits are characterized by complex stratigraphical relationships between hydromagmatic pyroclastics and lavas (related to M.Chirica and M.S.Angelo stratocones) and marine deposits, attributed to three different orders of ancient shorelines. These deposits are uniformly covered by post-Tyrrhenian pyroclastic successions (81-13 ka).

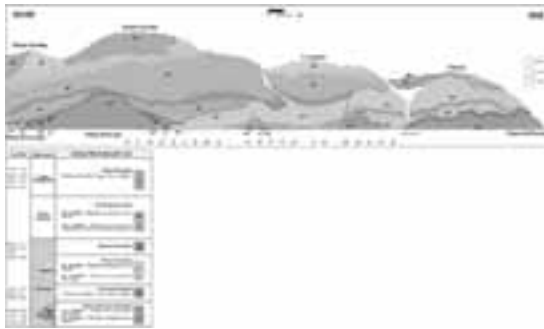


*Figure 27 - Shore-parallel vertical profile along the southwestern coast of Lipari, where a natural stratigraphic section is shown. In particular, the stratigraphic relationships between the three first phases of rhyolitic endogenous dome effusion are highlighted (pe1 = I phase; fa2 = II phase; gi2 = III phase). The domes are associated with the pumiceous pyroclastic layers relating to the corresponding explosive phases (pe2, fa1, gi1). The recurrent lavic domes and pyroclastics are interbedded with pyroclastic layers of exotic provenance, known as "Lesser Brown Tuffs" (pi = Pianoconte formation). (From Lucchi et al., 2004).*

**Stop 2.4:**

*Locality:* From Valle Muria to Lipari.

*Description:* Post-Tyrrhenian volcanics (81-13 ka). The stratigraphical relationships between different superimposed orders of rhyolitic domes and related pyroclastics will be observed, particularly at "Scogliera sotto il Monte", where a spectacular natural geological cross-section is exposed. Along this section the typical internal structures of rhyolitic endogenous domes (foliation and rampart structures) are visible. At Punta S.Giuseppe, a pit crater with resurgent dome is clearly visible.

**DAY 3**

**Lipari**

The third day will be devoted to illustrating the depositional facies, and facies evolution, of the deposits which characterized the younger volcanic

stratigraphy of the Island of Lipari. We will be leaving Lipari town eastwards, to look out at the domes structures and the proximalpyroclastic surge deposits of the Mt. Guardia sequence; afterwards, we will take the road which crosses the eastern coast of the island, to reach the northern sector of Lipari, where the youngest volcanic products crop out.

**The Monte Guardia lithosome**

An eruption of short duration produced thick pyroclastic deposits that lie between brown ash-flow tuffs, dated at 22,600 +/- 300 and 16,800 +/- 200 years ago (Crisci et al., 1981). The deposits cover Lipari Island, ranging in total thickness from more than 50 m just out of Monte Guardia, where the vent is located, to <1 m in the northern part of the island. The initial deposits are lithic-rich breccias, which are overlain by a series of lapilli fall deposits, and surge beds with wave-lengths from meters to tens of centimeters (fig. 28). Dry and wet fine laminated surge beds increase in frequency until the end of the eruption, when a viscous lava dome plugged the vent.



*Figure 28 - Low-angle cross-stratification in the upper wet and dry surges of the Mt. Guardia sequence.*

The deposits are dispersed to the north, with Mt. St. Angelo (nearly 600 m high) acting as a morphological barrier to the surge dispersal (Fig. 29).

The volume of erupted products was estimated to be 3.25x10<sup>8</sup> m<sup>3</sup> of lava, and 4.75x10<sup>8</sup> m<sup>3</sup> of pyroclastic materials (Sheridan et al., 1987). The total volume of dense magma erupted was estimated at close to 0.5 km<sup>3</sup>, of which about a half was emplaced as lava domes.

**The juvenile fraction: macroscopic description**

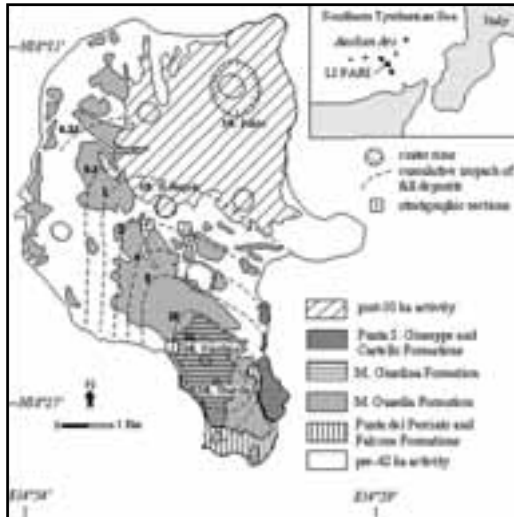


Figure 29 - Simplified geological map of Mt. Guardia products. From De Rosa et al., 2003 modified.

**and vertical variations in the deposits**

The pyroclastic deposits are mainly composed of juvenile glassy fragments, showing a wide variability in colour and texture.

De Rosa et al. (1993b) distinguished three main classes of juvenile fragments (white, grey, and streaky) (Fig.30). The white fragments (Fig. 30a,d) are mostly highly vesicular, elongated, «woody» pumice with low crystal content. Unaltered obsidian-like clasts occur, showing the same mineralogy of white pumice. The dense clasts may originate during interaction of magma with external water, since a hydromagmatic mechanism of fragmentation was operative during the Monte Guardia eruption (Crisci et al., 1981; De Rosa, 1999). Also, the obsidians may derive from the disruption of the chilled top of the magma column in the conduit, formed in the time between the explosive pulses (Crisci et al., 1981). This latter mechanism may account for the high abundance of obsidian clasts in some beds.

The grey pumice clasts are round-shaped, mildly vesicular, and with spherical vesicles (Fig. 30b,e). They display a large variation in colour within individual samples and between samples; as a general rule, the darker the colour, the more abundant the mafic phenocrysts in the pumice.

Streaky pumices show grey to dark grey bands alternating with white bands (Fig. 30c,f). Grey and banded clasts often contain brown rounded enclaves, a few cm in size at most.

The dark grey clasts, the banded clasts and the enclaves are most abundant at the bottom of the sequence; upwards, their abundance decreases and the grey clasts become lighter and lighter in colour. At the top of the coarse-grained fall deposits, 85 vol%

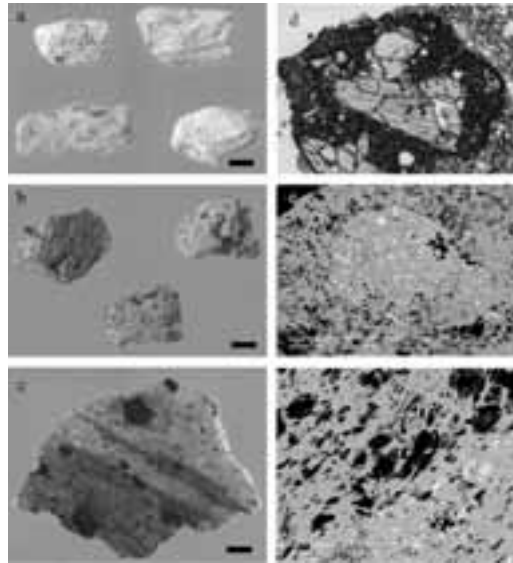


Figure 30 - a) and d): White pumice with tabular shape and elongated vesicles (bar =1cm) .b) and e): Grey pumice, rounded, poorly vesicular and crystal rich (bar=1cm). C) and f) Banded pumice characterized by mafic enclaves. From De Rosa et al., 2003.

of the juvenile fraction is made up of white juvenile components, and the remainder, of very light grey clasts (Fig. 31).

Microthermometry on melt inclusions and feldspar geothermometry (Wen and Nekvasil, 1994) indicates a temperature of crystallization of around 760°C for the Monte Guardia rhyolite. The mineral association and the presence of bivalent Europium indicate crystallization in conditions of low  $fO_2$ . The pre-eruptive content in dissolved  $H_2O$  is around 5 wt%, and was determined by FTIR on melt inclusions and by the plagioclase-melt equilibrium (Housh and Luhr, 1991), and is in accordance with the presence of unrimmed hornblende (Rutherford and Devine, 1988). Dissolved chlorine is about 3000 ppm, while  $CO_2$  and S are absent in the melt. These data indicate a P of crystallization of at least 200 MPa, or 6-8 km of depth. The data collected on the older Lipari rhyolites (42 ky) indicate the same conditions (Gioncada et al., 2003). The described pre-eruptive conditions characterize both the

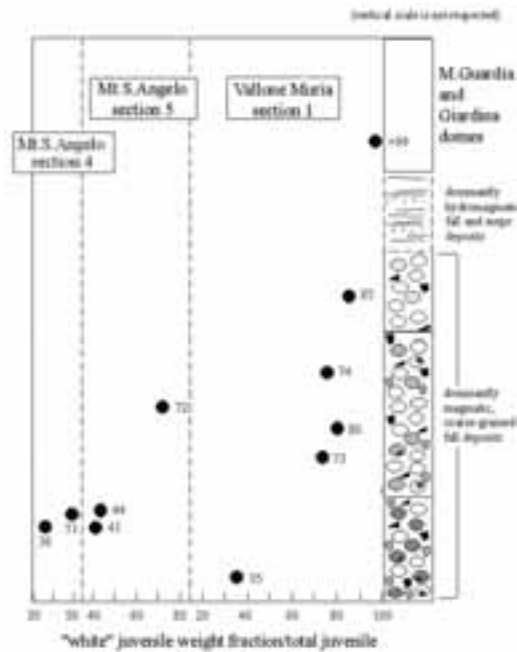


Figure 31 - Variation of the mixing proportions through the sequence of deposits of the Monte Guardia eruption. From De Rosa et al., 2003.

explosive activity and, at least in the initial phase, the effusive one.

**Factors controlling the possibility of fragmentation**

De Rosa et al. (1993b) suggest that the different rhyolites erupted at southern Lipari ascended from magmatic reservoirs located at medium depth (6-8 km), and that they had close to 5 wt% dissolved H<sub>2</sub>O. These features characterize magmas erupted explosively, with a magmatic and an hydromagmatic fragmentation mode, and effusively. Thus, the pre-eruptive volatile content does not represent here a main factor controlling the eruptive style of rhyolitic magmas. Syn-eruptive degassing during the rising of magma in the conduit (Eichelberger, 1995; Jaupart and Allegre 1991), may have been the governing factor on the shift from explosive to effusive style in the case of the Monte Guardia eruption. Gas loss during ascent may have been favoured by the rather low mass eruption rate at the beginning of the eruption (Woods and Koyaguchi, 1995), and by the pulsating character of the explosive phase. The increase in viscosity, due to the increase of the rhyolitic magma fraction which took place with the exhaustion of the mafic mixed magma, was a

main factor in determining the rapid decrease of the eruption rate, before the effect of the progressive emptying of the chamber took effect. The abundant obsidian clasts in the deposits come from the degassing magma along the conduit walls, and from devolatilization and cooling at the top of the magma column, in between successive explosive pulses (De Rosa et al., 2003c).

**The Vallone del Gabelotto lithosome**

The Gabelotto lithosome includes the deposits of the Gabelotto-Fiume Bianco tephra of Cortese et al. (1986), and the large endogenous obsidian-rich flowing dome of Pomiciazzo formation, dated at 11.4 and 8.6 ka respectively by fission-track determinations (Pomiciazzo lava; Bigazzi e Bonadonna,1973). The deposits cover an area of about 11km<sup>2</sup> within the 2m contour on the northern part of the island. The best outcrops lie in Gabelotto gorge and in the Fiume Bianco area where extensive quarrying has exposed excellent sections (Fig. 30 and 32).

The deposits consist of aphyric, rhyolitic pumices,



Figure 32 - Panoramic view of the Gabelotto products in the Gabelotto gorge.

obsidian clasts (<5%), and geothermal altered lava clasts (<5%). The sequence is formed by an alternation of fall and large-scale wavy bedforms of surge origin. The wavy beds show symmetrical and asymmetrical dune-forms, with minor antidune structures. Because a typical features of the surge deposits is the presence of bedsets which contain a coarse lower layer of pumice, that grades upwards into an overlying fine ash layer, Frazzetta et al. (1989), have proposed a new model for the emplacement of surge beds of this type. They assume that during high velocity transport, the coarser particles that fall into a moving surge cloud settle to its base. There they either remain in place as a ballistic fall population, or are swept along for a short distance in the traction carpet. These materials form

the coarse part of the bedset, while the finer material is either transported above the traction carpet, or trapped between the larger stationary pumice clasts. A large portion of the deposit has been moved by saltation or intermittent saltation. As the cloud slows, either with time, distance, or due to local flow perturbations, progressively smaller clasts settle into the traction carpet, where they are deposited together with the rolling coarse pumice. At the waning stages of the passage of a surge, and at more distal localities where the velocity is sufficiently slow, most of the coarse pumice has been deposited, and clasts transported by saltation and suspension form the capping horizon of the bedsets. A paired bedset thus represents the passage of a single surge cloud.

### The Mt. Pilato lithosome

The Mt. Pilato lithosome mainly includes the pumiceous succession which builds the cone of Mt. Pilato and the Fossa delle Rocche Rosse formation. Historical reports indicate the date of AD 729 for the latest volcanic activity (Cortese et al., 1986). The internal structure of the cone is clearly visible in the Campo Bianco and Acquacalda quarries (Fig. 33). The deposits mainly consist of pumiceous lapilli



Figure 33 - The internal structure of the Monte Pilato pumice cone (Campo Bianco quarry).

and bomb layers, alternating with pumice lapilli layers with abundant ash matrix in the middle part of the sequence. The top part consists of fine ash layers rich in accretionary lapilli, which alternate with rare pumice lapilli and bomb layers. Outside the cone structure, only the deposits that form this upper portion of the sequence crop out. In the inner crater zone, there is an erosional contact between the Monte Pilato sequence, and the deposits of Fossa delle Rocche Rosse formation, which consists of a 20 m thick coarse grained pumice strata, alternating with ash layers formed a small cone that subsequently was

partly covered, and partially destroyed, by the effusion of the obsidian lava flow of Rocche Rosse that ended the eruptive activity. Dellino and La Volpe (1995, 1996) identified four main lithofacies, representing 90% of the erupted products (Fig. 34).

These lithofacies include well-sorted pumice lapilli

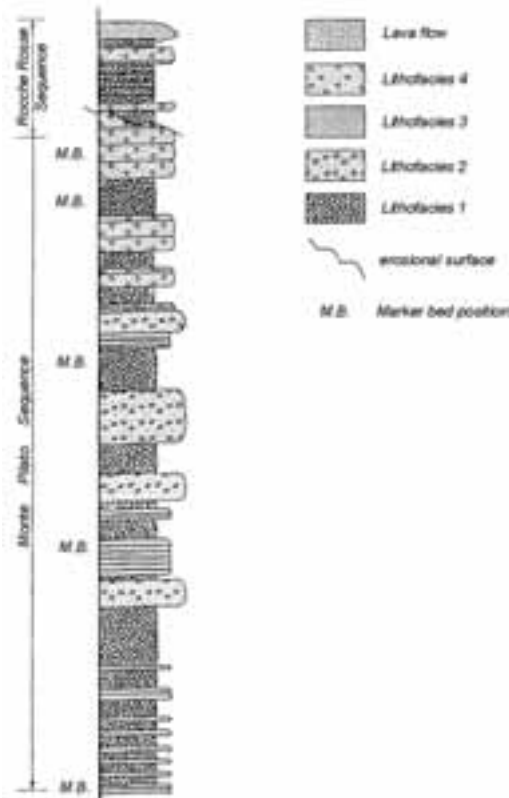


Figure 34 - Schematic composite stratigraphic section of Mt. Pilato-Rocche Rosse sequence (from Dellino and La Volpe, 1995).

graded beds of fall origin (lithofacies 1), poorly-sorted massive beds of flow origin (lithofacies 2), plane-parallel surge beds (lithofacies 3), and fine ash deposits with abundant accretionary lapilli (lithofacies 4). Field and laboratory data lead to the suggestion that during the Monte Pilato-Rocche Rosse eruptions, magmatic and hydromagmatic mechanisms occurred, frequently at the same time, and that both fallout and flow emplacement mechanisms were operative.

### General considerations

Rhyolites of Vallone Gabellotto, and Mt. Pilato lithosomes, lack any phenocrysts in equilibrium with the silicic glass, so we have no indications

on their pre-eruptive conditions. As a working hypothesis, De Rosa et al. (2003c) suggest that the absence of phenocrysts could be related, not to heating by a mafic magma that is never erupted, but to water-undersaturated isothermal decompression (Blundy and Cashman, 2001). They argue that, as an undersaturated magma ascends and P decreases, the temperature of liquidus will decrease at a rate of  $\sim 0.5^{\circ}\text{C}/\text{MPa}$  (Johannes and Holtz, 1996), and may become lower than the temperature of the magma, inducing crystal resorbing. Melting of crystals will dilute the  $\text{H}_2\text{O}$  dissolved, postponing  $\text{H}_2\text{O}$  saturation. During ascent,  $\text{H}_2\text{O}$ -saturation will be attained, and degassing will provokes the migration of the  $T_{\text{liquidus}}$  to higher values. The consequent undercooling will result in crystallization, except for highly viscous silicic melts, where it may be kinetically impeded. This may be what happened in the case of the Lipari aphyric rhyolitic products.

dome structure, which outcrops in the southeastern sector of Lipari (the 40m high and 200m wide, “low lava dome” of Blake, 1990). It represents the northermost extrusion of three endogenous lava domes which belong to the Punta S. Giuseppe lithosome (between 23.5 and 16.8 ka), and is aligned along a NNW-SSE direction. This dome consists of a sub-aphyric rhyolite containing variously deformed enclaves of latitic composition (Gioncada et al., 1993).



Figure 35 - Location of stops

**Stop 3.1:**

*Locality:* Near S. Anna

*Description:* Panoramic view of the Mt. Guardia and Mt. Giardina rhyolitic domes, as well as of the Mt. Guardia pyroclastic sequence. Close-up of the mingling structures and textures of the S. Nicola dome (Fig. 36).

The S. Nicola dome is a small asymmetrical-type



Figure 36 - Mafic enclaves of latitic composition included in the rhyolitic lava dome of S. Nicola.

**Stop 3.2:**

*Locality:* Vallone Muria

*Description:* The valley provides an excellent exposure of most of the Mt. Guardia sequence in a proximal area, where it is about 25m thick. The stop includes: 1) A panoramic view of the lowest coarse-grained beds, which are alternated with distinct fine-grained beds, that have been used as key markers to correlate the measured sections. 2) A close-up of the upper dry and wet surge deposits of the sequence.

**Stop 3.3:**

*Locality:* Near Lami village

*Description:* Close-up of the spatter pumiceous deposits of the Lami center. On the wall of the gorge, we will observe the sequence of the Vallone Gabelotto formation. In the lower part of the section pumice fall strata alternate with layers of surge origin. The surge sequence prevails in the upper part of the sequence, where the wave structures have an amplitude of 25 m.

**Stop 3.4:**

*Locality:* Acquacalda quarry

*Description:* A hundred meter-thick sequence of Mt. Pilato pumiceous deposits is exposed in this quarry.

The strata are mainly meter-thick layers of pumice bomb and ash, with scattered lithic clasts, which alternate with decimeter-thick layers of pumice lapilli. A significant part of the sequence can be interpreted as due to secondary volcanoclasti processes.

### Stop 3.5:

*Locality:* Fiume Bianco quarry

*Description:* Close-up of the Vallone Gabellotto sequence. The sequence shows wave-like bedforms with minor planar bedforms. Several of these layers form paired bedsets, with a coarse pumiceous lower part that grades upwards into overlying fine ash layers.

## DAY 4

### Vulcano

The Island of Vulcano is an active volcano of the Aeolian archipelago.

The whole subaerial part of the island was built up during the last 120ka, and consists of four main

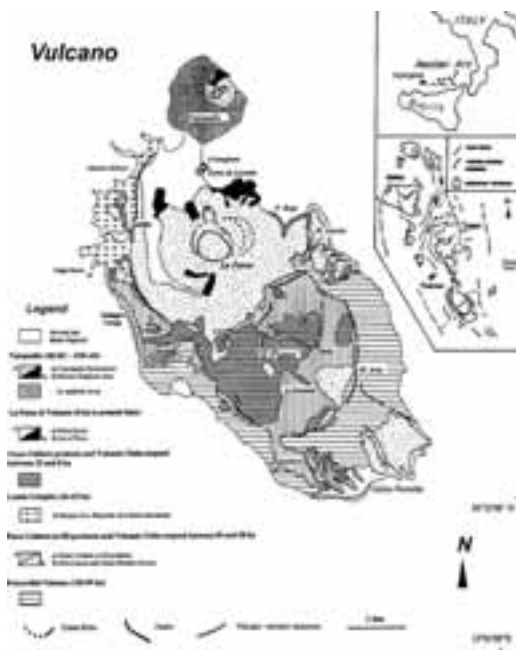


*Figure 37 - Geological sketch map of Vulcano Island, showing the distribution of the volcanic units erupted during the six main periods of activity (modified after De Astis, 1995). The top inset shows the location of the Aeolian archipelago in the Tyrrhenian Sea; the bottom inset represents a structural sketch map of the Vulcano-Lipari-Salina Islands (modified after Ventura, 1994)*

volcanic structures (Fig. 37): the South Vulcano centers, the Lentia complex, the Fossa cone and Vulcanello.

Two caldera-type structures are present in the central part of the island. The Caldera del Piano was formed (98 ka) by the collapse of the summit part of South Vulcano. This depression was infilled partially by compound lavas, and successively by pyroclastic deposits related to volcanic centers mostly located inside the caldera and along its rim. The present caldera floor has a mean altitude of 350m a.s.l., and the caldera rim reaches a maximum height of 500m a.s.l. The younger Caldera della Fossa depression was formed by large collapses affecting the northern sector of the Caldera del Piano and the Lentia volcanic complex during the last 50ka (Gioncada and Sbrana, 1991; Voltaggio, M. 1993 pers. comm.). The present floor of the depression has an altitude ranging from 7m (northern sector) to 172m (southern sector).

The La Fossa cone, which is the active volcanic edifice of the island, as made evident by the intense fumarolic emission, has developed inside the Caldera della Fossa depression. The subaerial part of the cone was formed in the last 6ka, and rests on the compound lava flows of La Roia (14ka). The Vulcanello peninsula was formed between the 2nd century B.C. and the 16th century A.D. in the northern sector of the island.

The last eruptions of Vulcano took place at the La Fossa cone in 1888-90 (and these were of the "vulcanian" type of eruptions).

*STRATIGRAPHY AND VOLCANOLOGY OF THE ACTIVE CONE OF*



*Figure 38 - Photograph showing the La Fossa cone and the walls of the La Fossa caldera of Vulcano.*

#### LA FOSSA

The stratigraphy of La Fossa di Vulcano has been studied at the centimeter scale, and beds due to each of the eruptive events of the volcanic history have

been distinguished (Dellino and La Volpe, 1997). The discontinuities identified in the stratigraphy have lead to the attribution of beds to individual eruptions, and to the grouping of eruptions into "Successions". Geochronological data have been used to support these subdivisions, and to delineate the timing of eruptions and quiescence periods. Following this scheme, five successions, which comprise a total of 14 eruptions, have been distinguished in the stratigraphy of La Fossa (Fig. 39).

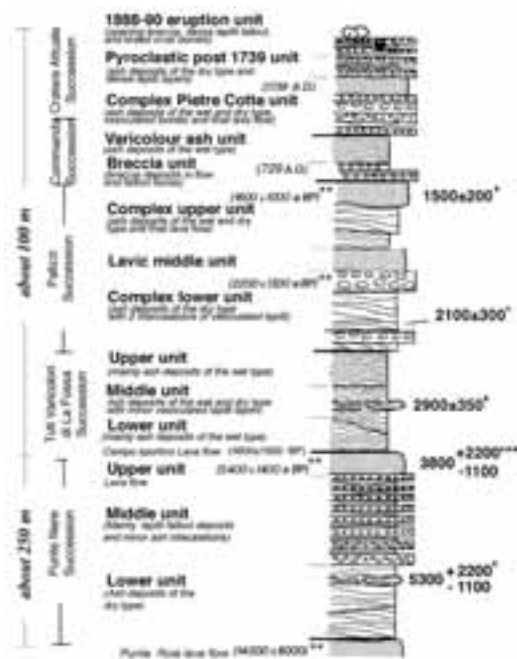


Figure 39 - Schematic stratigraphic section of the eruptive products of La Fossa di Vulcano. (modified after Dellino and la Volpe, 1997)

From the older to the younger one these five successions are: 1) the Punte Nere Succession, which encompasses 3 eruptions; 2) the Tuffi Varicolori Succession, which comprises 3 eruptions; 3) the Palizzi Succession, which has been formed by 3 eruptions; 4) The Commenda Succession, which is made up of 2 eruptions; and 5), the Cratere Attuale Succession, which has been characterized by three eruptions.

The Punte Nere Succession, whose deposits dispersal area is shown in fig 38a, represents the most part of the erupted material of the whole eruptive activity of La Fossa, and has lead to the edification of the main structure of the volcanic edifice. The successive eruptive activities have only emphasized or partly modified the cone form. This Succession

has been subdivided into three units that differ in the lithological characteristics of the deposits, and in the different dispersal areas of the products.

In the lower unit, latitic hydromagmatic dry deposits of ash prevail. They are the most dispersed deposits of the eruptive history of La Fossa. In the top part of these deposits, a metric layer of latitic welded scoriae, with a radiometric age of 5300±2200/-1100 years BP, is present. The deposits of this unit have formed a 150 meter-high tuff ring with a 15° slope angle. The intermediate unit is composed of dense lapilli and block deposits, due to ballistic fallout, in decimeter to meter-thick layers, which alternate with hydromagmatic ash layers. The deposits of this unit have an inclination of 30° and due to their accumulation, the volcanic cone reaches a height

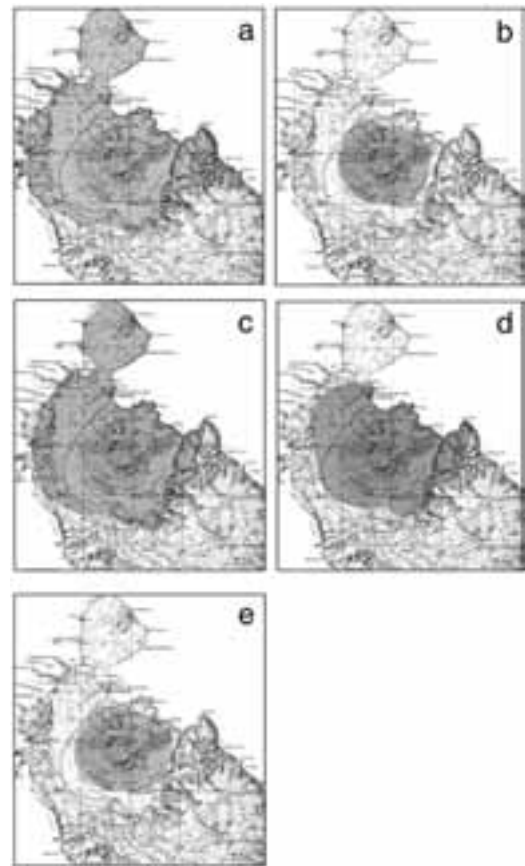


Figure 40 - Maps representing the dispersal area of the eruptive products of the 5 Successions of La Fossa di Vulcano. a= Punte Nere Succession; b= Tuffi Varicolori Succession; c= Palizzi Succession; d= Commenda Succession; e= Cratere Attuale Succession (modified after Dellino and la Volpe, 1997).

of about 250 m. The upper unit is represented by a trachitic lava flow, with a radiometric age of  $3800 \pm 2200$ /-1100 years BP.

The second succession, whose deposits dispersal area is shown in Fig 40b, Tufi Varicolori di La Fossa, has been subdivided into three units that are separated by erosional surfaces. These three units have similar lithological characteristics and dispersal area. The lower and upper units are made up mainly of hydromagmatic ash deposits, whereas the intermediate one is composed of a sequence of latitic and shoshonitic ash layers, with some intercalations of shoshonitic layers of vesiculated lapilli and bombs due to ballistic fallout. One of the latter has a radiometric age of  $2900 \pm 350$  years BP.

The third succession, whose deposits dispersal area is shown in Fig. 40c, Palizzi, has been subdivided into three units based on the occurrence of erosive surfaces. The lower complex unit is made up of a sequence of hydromagmatic ash deposits, with two intercalations of vesiculated lapilli and bombs due to ballistic fallout. The first one has a rhyolitic composition, the second, trachitic. One of the ash beds has a radiometric age of  $2100 \pm 300$  BP. The intermediate unit consists of a lava flow that surrounds the eruptive vent, and has flowed only a few hundred meters from the emission crater. The upper complex unit, formed about 1500 years BP, is made up of a sequence of hydromagmatic ash deposits, and by a trachitic lava flow that extends southwards down to the cone base.

The fourth succession, the Commenda succession, whose deposits dispersal area is shown in Fig. 40d, was formed about 1250 years BP. It is made up of a breccia unit at its base. It is composed of a metric layer of dense lapilli and blocks set in an ash matrix, by a dense lapilli and blocks layer due to ballistic fallout and by an ash layer. These deposits are mainly composed of lithic clasts showing a high degree of hydrothermal alteration. After a brief period of rest, the varicolori ash unit formed. It is mainly composed of a densely- stratified sequence of latitic hydromagmatic ash deposits. They are the most widespread deposits of the whole Commenda succession.

The fifth succession, whose deposits dispersal area is shown in Fig. 40e, the Cratere attuale one, has been subdivided into three units, taking into consideration both stratigraphic features and eruptions chronicles. The complex unit of Pietre Cotte is composed at the base of latitic hydromagmatic ash deposits. A metric vesiculated lapilli and bombs deposit, due to ballistic fallout of rhyolitic composition comes after the Pietre

Cotte rhyolitic lava flow, which was effused in 1739 AD on the eastern sector of the cone, and closes the unit. The deposits of this unit are dispersed around the cone.

The post 1739 unit is made up of an alternation of hydromagmatic ash layers and dense lapilli and blocks deposits due to ballistic fallout. It has been formed by periodic and intermittent eruptive activity. The eruption chronicles reports that in the period 1739 – 1888, frequent eruptive events occurred. The dense lapilli and block deposits have a dispersal area restricted to the volcanic edifice, whereas isolated outcrops of some layers of hydromagmatic ash have been found outside the cone, on the Caruggio area, and also outside the rim of the La Fossa caldera, both at the Lentia complex, and at the base of Monte Saraceno. The 1888-90 eruption unit is formed by a sequence of dense lapilli and blocks deposits, with intercalations of hydromagmatic ash layers. A layer of vesiculated lapilli and bombs of latitic composition is also present within this sequence. Dense clasts of lapilli and blocks with scattered bread crust bombs, represent the products of the last eruptive

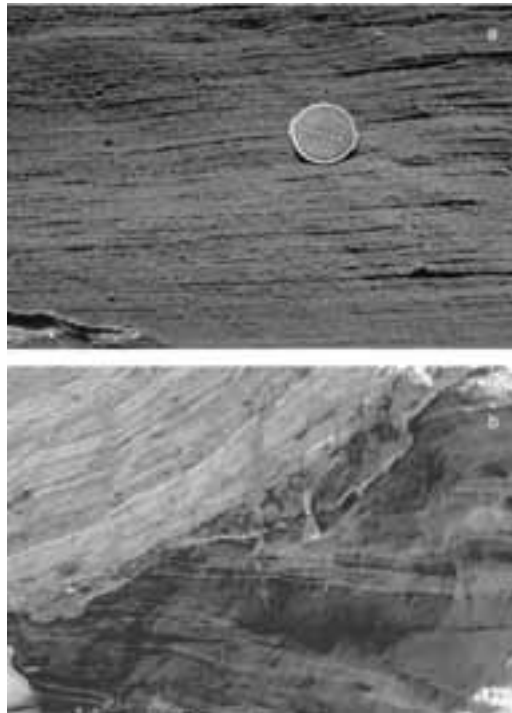


*Figure 41 - a= Photograph showing a close-up view of a dry surge bed of La Fossa di Vulcano; b= photograph showing the contrasting lithological features of dry surge (top) and wet surge (bottom), deposited at La Fossa di Vulcano.*



Figure 42 - Photograph showing a close-up view of centimeter-thick wet surge beds of La Fossa di Vulcano.

event. These clasts, up to several meters big in the crateric area, have a relatively large dispersion area around La Fossa cone.

**Hydromagmatic deposits of La Fossa**

Using a scheme based on thickness, grain size and structure, beds of the whole stratigraphic sequence of La Fossa have been grouped into 5 lithofacies each of which represent deposits due to similar fragmentation and transportation dynamics. Among these lithofacies the most recurrent one, constituting more than 80% of layers is made up of centimeter to decimeter-thick ash layers that were emplaced by turbulent and dilute flows (surge). These deposits are related to hydromagmatic eruptive processes. As the result of the explosion and fragmentation, due to effective magma/water interaction, ash particles were expelled out of the vent, together with gases and vapors. A «low angle» eruptive cloud was thus formed, and it fed gravity flows that expanded radially from the volcano. Because of the scarcity of lithic fragments, the hydromagmatic fragmentation at La Fossa di Vulcano probably occurred at very superficial levels in the conduit. Only for the deposits of the Punte Nere and Tufi Varicolori successions, which show a limited amount of lithic clasts, the fragmentation level has been a little deeper in the conduit.

These hydromagmatic ash deposits are distinguished into two sub-types, dry and wet (fig 41 and 42).

The difference between the two is due to the presence of a significant amount of condensing water during transportation, for the wet type. In the dry type the vapor was superheated instead. This difference is reflected in the structural and textural features of deposits. The dry deposits are coarser grained than the wet ones (fig. 43).

In the dry ones, the deposition is simply of the

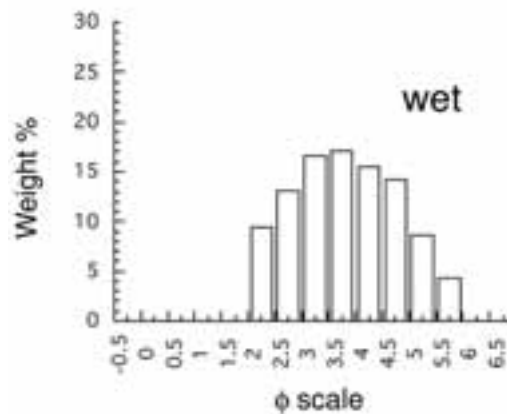
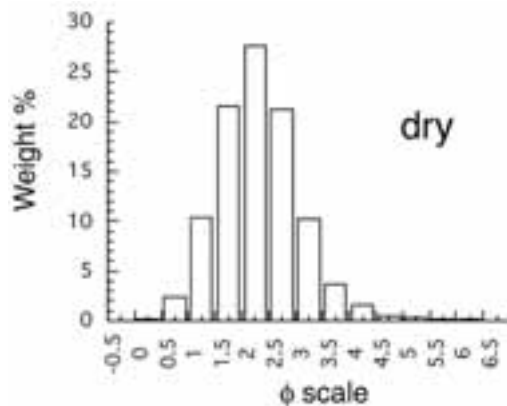


Figure 43 - Grain-size distribution of representative dry surge (a) and wet surge (b) beds.

tractional type and deposits typically occur as decimeter-thick layers which show inclined internal lamination (fig. 44).

In the wet ones, deposition occurs by water



Figure 44 - General view of dry surge beds of the Palizzi eruptions, showing a laminated structure and tractional features.

condensation, and there is a consequent aggregation of fine ash at the flow base. Deposits are centimeter-thick depositional units, with minor tractional structures, and typically show features such as accretionary lapilli, vesiculated tuffs, and plastic deformations (fig. 45), which reflect the presence of liquid water at the onset of deposition.

To make a hard and fast distinction between the



Figure 45 - General view of wet surge beds of the Commenda eruption, showing plastic type deformations induced by ballistic impacts.

structural and textural features of these two types of deposits is to refer only to the emplacement mechanism. In fact, it must be remembered that a continuous spectrum between the two types exists; inside the deposit sequences where the dry type prevail, some layers of the wet type are present too, and, conversely, in the wet sequences, some dry layers are always intercalated.

#### Fragmentation mechanisms

The phreatomagmatic activity of La Fossa was experimentally simulated with the use of the TEE-II Experiment at the Physikalisch Vulkanologisches Labor at Wuerzburg University (Buttner et al, 1999). A suitable magma simulant was generated by remelting the actual volcanic rock. Different experimental series were performed, simulating both wet and dry conditions, and in all cases 0.4 kg of melt at magmatic temperatures was prepared under atmospheric conditions and controlled oxygen fugacity in cylindrical crucibles. The experimentally produced wet and dry pyroclasts were then analyzed and compared to their natural analogues.

The size fraction containing the relevant information on the explosive magma/water interaction processes is the fine ash fraction.

Fine ash clasts derived from explosion

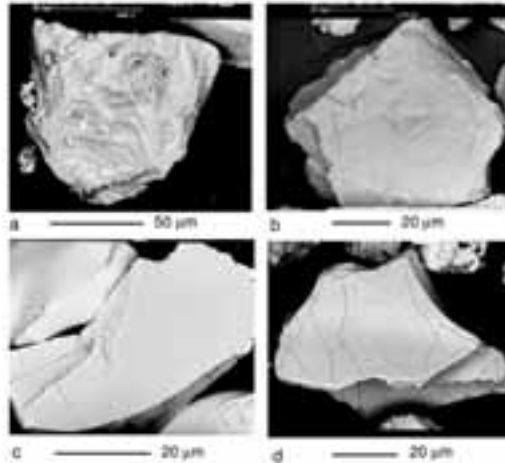


Figure 46 - Comparison between characteristic particles from experiments with those from natural deposits of La Fossa di Vulcano, using scanning electron microscope images.

- a, Blocky and equant-shaped particle from 'dry' explosion experiment (series I) with stepped surfaces and etches on the surface.
- b, Analogue particle from a 'dry' wet' explosion experiment (series II,) showing addition branching quench-crack structures.
- d, Analogue particle from a 'wet' phreatomagmatic surge deposit of La Fossa.

experiments of the dry type (series I) typically show blocky, equant shapes, and "stepped" glass surfaces by "mechanical" etching (fig. 46a). The same type of particles are present in the fine ash fraction of natural dry and wet deposits (fig. 46b). These clasts obviously result from a brittle process, i.e. the deformation rate acting on the magma was so high, that liquid relaxation of the stresses could not work. These particles have been identified as the fingerprints of thermohydraulic explosion processes, representing the most intensive type of magma/water interaction. Fine ash fragments from explosion experiments of the wet type (series II), show similar features, plus, on a significant number of fragments, the glass surfaces are covered by a branching network of quench cracks (Figure 46c). These cracks must have formed immediately after fragmentation, due to sudden cooling. These kind of clasts are also found in natural phreatomagmatic deposits (Figure 46d), and in significantly higher amounts in wet surge deposits compared to the dry ones. These quenching structures, that were never found in the products of the dry experiments (series I), are related to the fast passage of just fragmented particles through a domain of liquid water. This

mechanism results in a high cooling rate and thus in an effective chilling. Particles of this kind only form when excess water is present in the conduit, and they are more frequent in the wet than in the dry phreatomagmatic deposits of La Fossa.

The quench crack structures, exclusively observed on the surfaces of ash grains produced by explosive magma/water interaction under wet conditions, are actually the record of wet explosive phreatomagmatic volcanism to be found in pyroclastic deposits of ancient and recent eruptions. The occurrence of a minor amount of these kind of marker particles in the so-called dry surge deposits of La Fossa thus indicates, that also in this case a moderate amount of excess water was present during the eruption.

#### Transportation and deposition mechanisms

What is very important in the study of ash deposits due to turbulent and diluted flows, is not the deposit "as is", but the flow that produces it. It is the flow that represents the danger to human life of these type of eruptive events. As opposed to the fallout deposits, where the danger is related to the load of the deposit on the roofs of houses, in the case of turbulent and diluted flows, it is the velocity, thickness, temperature, and toxicity of the flow which determines how hazardous it is.

Actually, in the case of the dry type of flows, the fine particles are always held in a turbulent suspension, and they are deposited only when the flow, in its final stages, drops significantly in velocity.

In the case of the wet type, in the basal portion of the flow (in contact with the substratum) where the viscous forces prevail, the vapor is more abundant, and is effectively cooled and aggregates the fine particles, to form the peculiar structures of these type of deposits. The overlying part of the flow, which does not experience the viscous effect that occurs at the base, continues to move as a turbulent and diluted flow, but will not be able to induce very significant tractional effects on the just-deposited material, because fine, adhesive particles show a very high resistance to tractional movement. The dynamics of transportation of the flows of the wet and dry types are indeed analogous, only the emplacement model is different.

Since for the hazard assessment of these type of events, the dynamics of the flow are important and not the deposit "as is", let's see what kind of information we can gain on this subject, by using

the structural features of the deposits at La Fossa di Vulcano.

The following lateral variations of structural and textural features along two directions that form the Fossa cone, and which cross the obstacle barrier of the Caldera di la Fossa, give important insights into the flow characteristics.

Along the profile that goes from the crater to Monte Rosso (Fig. 47), the deposits laterally pass from a laminated structure, at the base of the cone, to a massive, high structure beneath the steep morphological barrier of the caldera.

We can indeed affirm that because the flow had a thickness not significantly in excess of the height of

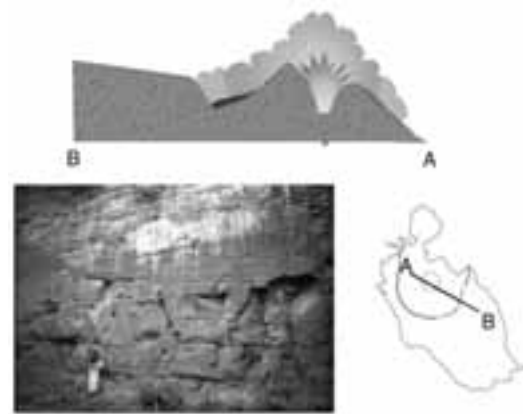


**Figure 47 - Depositional behaviour of surge deposits that laterally pass from a laminated to a massive structure which causes a steep topographical jump.**

the morphological obstacle, it therefore experienced a strong deceleration, and the solid material was suddenly deposited and the flow, losing its load of particles, was extinguished.

In the second case (Fig. 48), which represents the profile that goes from the crater to Piano di Alighieri, the deposits always show a laminated structure.

This means that the flow had, along that direction, a thickness high in excess of the morphological obstacle, and therefore did not experience sudden decreases in velocity, and we can conclude that at Piano di Alighieri, the flow was still expanded, and that the velocity was high enough (tens of m/sec) as to produce tractional features on the deposited material. Therefore, even if we do not find significant outcrops over Piano di Alighieri (because they were successively eroded), the flow, with its residual load of particles, has travelled even further south, as far as

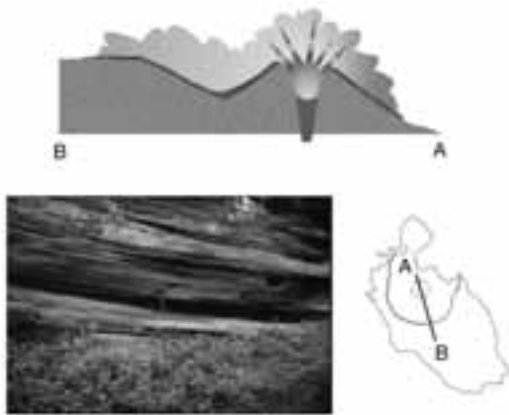


**Figure 48 - Depositional behaviour of surge deposits that maintain a laminated structure also when surpassing a topographic barrier.**

the Piano Area.

This situation occurs for the deposits of the Punte Nere, Palizzi, and Commenda succession, where, as a function of the local height and morphology of the caldera rim, the deposits in some locations suddenly pass from laminated to massive structures, whereas in other locations they remain always laminated, again in correspondence to the caldera rim and its flanks.

Concerning the deposits of the post 1739 unit of the Cratere attuale succession, it is not possible continuously to follow the lateral structural evolution, but since the depositional units found at the base of Monte Saraceno have tractional structures, it is possible to suggest for these events as well, that the flows have surpassed the caldera rim and have expanded throughout the Piano Area.

Using this evidence as a starting point, the loose ash that covers the Piano area has been analyzed, and it has been possible to attribute it to La Fossa activity, in particular to the Palizzi eruptions (Dellino and La Volpe, 2000).

Based on this evidence, a sedimentological study has been carried out on the turbulent and diluted flows, using the structural and textural features of those deposits which, on showing lateral continuity, allowed the testing of results.

Deposits from the Palizzi eruptions have been chosen because it was possible to continuously trace correlated layers from the base of the cone to over the La Fossa caldera rim. The results of the application of the sedimentological model indicates

that at the base of the cone, flows had a velocity in excess of 50 m/sec, and a thickness in the order of 280 meters. The part of the flow that surpassed the caldera barrier was about 90 meters thick, and had a velocity of about 30 m/sec. The distance the ash particles travelled in turbulent suspension before the flow was extinguished, was in the order of 1100 meters from Passo del Piano, which is the topographical opening from which flows have repeatedly overridden the caldera obstacle in the past. This distance is in agreement with the dispersal area of the loose ash that covers the Piano Area and has been attributed to the Fossa activity. The converging geological and sedimentological results demonstrate that the model proposed, even if it is approximate, adequately describes the fluidodynamics of the turbulent and diluted flows of ash, and that this model might help to predict the turn of events at La Fossa di Vulcano in any future eruption.

#### **Hazard assessment**

The sedimentological model used for the reconstruction of the fluid-dynamic characteristics of the flows, takes into consideration deposits, from a single eruptive event which emits about 1 million cubic meters of material out of the vent. For these type of events, an approximate calculation of the water needed to produce the hydromagmatic explosion, is in the order of tens of thousands of cubic meters. This estimation comes from calculations based on experimental data.

The elaboration of a deterministic model of the hazard related to the expected event, will be possible only on the basis of a detailed knowledge of the hydrogeological system of La Fossa di Vulcano, which will allow the exact determination of the amount of water available in the conduit system, at the onset of the eruption. The forecast of such an event is related to the ability of geophysical and/or geochemical methods to record the rate of ascent of such volumes of magma in the superficial level of the conduit.

It is possible to give a probabilistic estimation of the hazard related to the expected event, taking into consideration the data obtained from both the eruptive scenario, and the sedimentological model.

In the hazard assessment, the eruptive events that characterized the eruptions that occurred during and after the Palizzi succession, can be considered, since the previous ones had characteristics that seem

unlikely to be repeated in the future.

**In 50% of the eruptions that occurred, starting from the Palizzi succession, the flows have surmounted the La Fossa caldera rim. The flows, at the base of the cone (in the Palizzi area), had a maximum velocity in excess of 50 m/sec. Due to the radial dispersal area, this is the velocity that we have to expect at Vulcano Porto in a future eruption. With this velocity, and relative flow thickness and concentration, the flows will cross the whole Vulcanello area, with all their destructive power in terms of loss of human life. These flows will likely surpass the La Fossa caldera rim with maximum velocities, in the order of 30 m/sec, and maintain their destructive effects in the zone of Piano di Alighieri. The area, onland, which is affected by these flows, is**

**colored in light grey on Fig. 49, and represents a 50% of hazard.**

In 75% of the eruptions, these kind of events have flowed with a velocity of tens of m/sec and with a high expansion, and also travel over the Caruggio area. Considering a radial dispersal, these flows also cross the whole Volcanello area. The area in medium grey in Fig. 49, envelopes the events of this magnitude and represents a 75% chance of hazard occurring.

In the 100% of cases the flows have expanded over the base of the cone of La Fossa, with their accompanying hazardous effects. The area in dark grey of Fig. 20 represents such a kind of event, and represents 100% chance of hazard occurring.

The Gelso area, and the road that goes from Piano to Gelso, is considered to be safe. In these localities, the hazard of the expected event is avoided, because of the sharp hydraulic jump that causes the sudden expansion downslope of the flow. On these flows, highly diluted in origin, a further dilution produces the rapid decoupling of the basal and coarser load, from the overlying flow. The basal part will be immediately deposited, and the upper one will disperse in the atmosphere, to eventually settle on the ground very slowly.

The fourth day will be spent on the Island of Vulcano, where the active cone of Fossa is located. Proceeding along the road to the Piano, we will take a trail on the left to reach the top of the main cone.



*Figure 49 - Hazard map of La Fossa of Vulcano. The light grey area represents the zone where there is a 50% probability that flows will have impact in a future eruption. The medium grey area represents the zone where there is a 75% probability that flows will have impact in a future eruption. The dark grey area represents the zone where there is a 100% probability that flows will have impact in a future eruption.*



*Figure 50 - Location of stops.*

### Stop 4.1:

*Locality:* Gran Cratere rim

*Description:* A panoramic view of the Caldera della Fossa and of the surrounding volcanoes. Close-up observation of the 1888-90 products.

### Stop 4.2:

*Locality:* Palizzi

*Description:* Close-up examination of the deposits of the Palizzi eruptions, which represent the highest magnitude of events expected in the future at Vulcano. Facies analysis of some peculiar dry-surge beds will be carried out.

### Stop 4.3:

*Locality:* Lentia

*Description:* This outcrop illustrates: 1) the downcurrent facies evolution of the Palizzi surges, that are here mostly represented by fine-laminated grey beds, that commonly show low-angle oblique stratification. 2) the erosional contact with the lowermost deposits.

### References cited

- Allard, P., Aiuppa, A., Loyer, H., Carrot, F., Gaudry, A., Pinte, G., Michel, A. and Dongarrà, G. (2000). Acid gas and metal emission rates during long-lived basalt degassing at Stromboli volcano. *Geophysical Research Letters* 27, 1207-1210.
- Allard, P., Carbonnelle, J., Métrich, N., Loyer, H. and Zettwoog, P. (1994). Sulphur output and magma degassing budget of Stromboli volcano. *Nature* 368, 326-330.
- Antonioli, F., Cremona, G., Immordino, F., Puglisi, C., Romagnoli, C., Silenzi, S., Valpreda, E., Verrubbi, V. (2002). New data on the Holocene sea level rise in NW Sicily (Central Mediterranean Sea). *Global and Planetary Change*, 34/1-2, pp. 121-140.
- Barberi F, Gandino A, Gioncada A, La Torre P, Sbrana A, Zenuchini C (1994) The deep structure of the Eolian arc (Filicudi-Panarea-Vulcano sector) in light of gravity, magnetic and volcanological data. *J Volcanol Geoth Res* 61: 189-206.
- Barberi, F., Rosi, M. and Sodi, A. (1993). Volcanic hazard assessment at Stromboli based on review of historical data. *Acta Vulcanologica* 3, 173-187.
- Barker D.S., 1987. Rhyolites contaminated with metapelites and gabbro, Lipari, Aeolian Islands, Italy: products of lower crustal fusion or of assimilation plus fractional crystallization? *Contrib. Mineral. Petrol.*, 97, 460-471.
- Beccaluva L., Gabbianelli G., Lucchini F., Rossi P.L. and Savelli C. (1985) Petrology and K/Ar ages of volcanic dredged from the Aeolian seamounts: implications for geodynamic evolution of the Southern Tyrrhenian basin. *Earth Planet. Sci. Lett.*, 74, 187-208.
- Beccaluva L., Rossi P.L. and Serri G. (1982). Neogene to recent volcanism of the southern Tyrrhenian-sicilian area: implications for the geodynamic evolution of the Calabrian Arc. *Earth Evol. Sci.*, 3, 222-238.
- Bertagnini, A., Coltelli, M., Landi, P., Pompilio, M. and Rosi, M. (1999). Violent explosions yield new insights into dynamics of Stromboli volcano. *EOS* 80, 635-636.
- Bigazzi G. & Bonadonna (1973). Fission track dating of the obsidian of Lipari Island (Italy). *Nature*, 242, 322-323.
- Blake, S., 1990. Viscoplastic models of lava domes. In Jonathan H. Fink (Ed.) *Lava Flows and Domes, Emplacement Mechanisms and Hazard Implications*. Springer Verlag, Berlin. pp 88-126.
- Blundy, J., Cashman K. (2001) Magma ascent and crystallization at Mount St. Helens, 1980-1986 *Contributions to Mineralogy and Petrology* 140: 631-650.
- Bonaccorso A., Calvari S., Garfi G., Lodato L., Patanè D. (2003). Dynamics of the December 2002 flank failure and tsunami at Stromboli volcano inferred by volcanological and geophysical observations. *Geoph. Res. Lett.*, v.30, no.18, doi: 10.1029/2003GL017702.
- Bonaccorso, A., Cardaci, C., Coltelli, M., Del Carlo, P., Falsaperla, S., Panucci, S., Pompilio, M. and Villari, L. (1996). Annual report of the world volcanic eruptions in 1993, Stromboli. *Bulletin of Volcanic Eruptions* 33, 7-13.
- Bordoni, P., Valensise, G. (1998). Deformation of the 125 Ka marine terrace in Italy: tectonic implications. In: Stewart, I.S., Vita-Finzi, C. (Eds.), *Coastal Tectonics*, Geological Society, London, Special Publications 146, pp. 71-110.
- Büttner R., Dellino P., & Zimanowski B. (1999) Identifying modes of magma/water interaction from the surface features of ash particles. *Nature* 401, 688-690.
- Calanchi N., De Rosa R., Mazzuoli R., Rossi P.L., Santacroce R., Ventura G., (1993). Silicic magma

- entering a basaltic magma chamber: eruptive dynamics and magma mixing-an example from Salina (Aeolian islands, Southern Tyrrhenian Sea). *Bull. of Volcanol.*, 55, 504-522.
- Calanchi N., Capaccioni B., Martini M., Tassi F., Valentini L., 1995a. Submarine gas-emission from Panarea Island (Aeolian Archipelago): distribution of inorganic and organic compounds and inferences about source conditions. *Acta Vulcanol.*, 7(1), 43-48.
- Calanchi N., Romagnoli C., Rossi P.L., 1995b. Morphostructural and some petrochemical data from the submerged area around Alicudi and Filicudi volcanic islands (Aeolian Arc, Italy). *Mar. Geol.*, 123, 215-238.
- Calanchi N., Peccerillo A., Tranne C.A., Lucchini F., Rossi P.L., Kempton P., Barbieri M., Wu T.W., 2002a. Petrology and geochemistry of volcanic rocks from the Island of Panarea: implications for mantle evolution beneath the Aeolian island arc (southern Tyrrhenian sea). *J. Volcanol. Geotherm. Res.*, 115, 367-395.
- Calanchi N., Lucchi, F., Pirazzoli, P., Romagnoli, C., Tranne, C.A., Radtke, U., Reyss, J.L., Rossi, P.L. (2002b). Late-Quaternary and recent relative sea-level changes and vertical displacements at Lipari (Aeolian Islands). *Journal of Quaternary Science* 17 (5-6), 459-467.
- Chappell, J., Omura, A., Esat, T., McCulloch, M., Pandolfi, J., Ota, Y., Pillans, B. (1996). Reconciliation of late Quaternary sea levels derived from coral terraces at Huon Peninsula with deep sea oxygen isotope records. *Earth and Planetary Sciences Letters* 141, 227-236.
- Chappell, J., Shackleton, N.J. (1986). Oxygen isotopes and sea level. *Nature* 324, 137-140.
- Chiocci F.L. & Romagnoli C. (2002). Terrazzi deposizionali sommersi nelle Isole Eolie. In: "Atlante dei terrazzi deposizionali sommersi lungo le coste italiane" (a cura di F.L.Chiocci, S.D'Angelo, C.Romagnoli). *Mem. Descrittive della Carta Geologica d'Italia*, vol.58, in press.
- Continisio R., Ferrucci F., Gaudiosi G., Lo Bascio D., Ventura G. (1997). Malta Escarpment and Mt.Etna: early stages of an asymmetric rifting process? Evidences from geophysical and geological data. *Acta Vulcanol.*, 9, 39-47.
- Cortese, M., Frazzetta, G., La Volpe, L. (1986). Volcanic history of Lipari (Aeolian Islands) in the last 10.000 years. *Journal of Volcanic and Geothermal Research* 27, 117-133.
- Crisci, G.M., Delibrias, G., De Rosa, R., Mazzuoli, R., Sheridan, M.F. (1983). Age and petrology of the Late-Pleistocene Brown Tuffs on Lipari, Italy. *Bulletin of Volcanology*. 46-4, 381-391.
- Crisci G.M., De Rosa R., Esperanca S., Mazzuoli R., Sonnino M. (1991). Temporal evolution of a three component system: the Island of Lipari (Aeolian Arc, southern Italy). *Bulletin of Volcanology* 53, 207-221.
- De Astis G., Dellino P., De Rosa R., La Volpe L. (1997). Eruptive and emplacement mechanisms of fine grained pyroclastic deposits widespread on Vulcano Island. *Bull. Volcanol.*, 59, 87-102.
- De Astis, G., Peccerillo, A., Kempton, P.D., La Volpe, L., Wu, T.W. (2000) Transition from calc-alkaline to potassium-rich magmatism in subduction environments: geochemical and Sr, Nd, Pb isotopic constraints from the Island of Vulcano (Aeolian arc) *Contributions to Mineralogy and Petrology* (139), Issue 6, 684-703
- De Astis, G., La Volpe, L., Peccerillo, A., Civetta, L. (1997). Volcanological and petrological evolution of Vulcano Island (Aeolian Arc, Southern Tyrrhenian Sea). *J. Geoph. Res.* 102, B4, 8021-8050.
- De Astis G. F., Ventura G., Vilaro G., 2003, Geodynamic significance of the Aeolian volcanism (Southern Tyrrhenian Sea, Italy) in light of structural, seismological and geochemical data. *Tectonics*, 22, 4, DOI:10.1029/2003TC001506.
- Dellino P and La Volpe L. (1995). Fragmentation versus transportation mechanisms in the pyroclastic sequence of Monte Pilato-Rocche Rosse (Lipari, Italy). *Jour. Volcanol. Geotherm. Res.*, 64, 211-231.
- Dellino P and La Volpe L. (1996). Image processing analysis in reconstructing fragmentation and transportation mechanisms of pyroclastic deposits. The case of Monte Pilato-Rocche Rosse eruptions, Lipari (Aeolian Islands, Italy). *Jour. Volcanol. Geotherm. Res.*, 71, 13-29.
- Dellino, P. & La Volpe, L. (1997) Stratigrafia, dinamiche eruttive e deposizionali, scenario eruttivo e valutazioni di pericolosità a La Fossa di Vulcano. In: "CNR-GNV Progetto Vulcano 1993-1995 " L. La Volpe, P. Dellino, M. Nuccio, E. Privitera & A. Sbrana (Ed), Felici, Pisa. 214-237.
- Dellino P. & La Volpe L. (2000) Structures and grain size distribution in surge deposits as a tool for modelling the dynamics of dilute pyroclastic density currents at La Fossa di Vulcano (Aeolian Islands, Italy). *J. Volcanol. Geoth. Res.* 96, 57-78.
- De Fino, M., La Volpe, L., Falsaperla, S., Frazzetta, G., Neri, G., Francalanci, L., Rosi, M. and Sbrana,

- A. (1988). The Stromboli eruption of December 6, 1985-April 25, 1986: volcanological, petrological and seismological data. *Rendiconti Società Italiana Mineralogia Petrologia* 43, 1021-1038.
- De Rosa R (1999) Compositional modes in the ash fraction of some modern pyroclastic deposits: their determination and significance. *Bull. Volcanol.* 61: 162-173
- De Rosa R. & Sheridan M.F., 1983, Evidence for magma mixing in the surge deposits of the Monte Guardia sequence, Lipari. In Explosive Volcanism, M.F. Sheridan and F. Barberi eds., *Jour. Volcanol. Geotherm. Res.*, 17, 313-328.
- De Rosa R., Donato P., Gioncada A., Masetti M. & Santacroce R., (2003b). The Monte Guardia eruption (Lipari, Aeolian Islands): an unusual example of magma mixing sequence. *Bull. Volcanol.*, DOI: 10.1007/s00445-003-0281-2.
- De Rosa R., Donato P., Gioncada A., Mazzuoli R., Santacroce R. (2003c). Scenari eruttivi delle eruzioni riolitiche del settore centrale eoliano: stato delle conoscenze. *GNV, General Assembly*, june 9-11, p.236.
- De Rosa R., Frazzetta G., La Volpe L., 1992, An Approach For Investigating The Depositional Mechanism Of Fine-Grained Surge Deposits. The Example Of The Dry Surge Deposits At "La Fossa Di Vulcano". *Jour. Volcanol. Geotherm. Res.*, 51, 305-321.
- De Rosa R., Guillou H., Mazzuoli R. and Ventura G. (2003a). New unspiked K-Ar ages of volcanic rocks of the central and western sector of the Aeolian Islands: reconstruction of the volcanic stages. *Jour. Volcanol. Geotherm. Res.*, 120, 161-178.
- De Rosa R., Mazzuoli R., Ventura G., 1996, Relationships between deformation and mixing processes in lava flows: a case study from Salina (Aeolian Islands, Tyrrhenian Sea). *Bull. of Volcanol.* 58, 286-298.
- Eichelberger, J.C. (1975) Origin of andesite and dacite: evidence of mixing at Glass Mountain in California and other circum-Pacific volcanoes. *Geol Soc Am Bull* 86: 1381-1391.
- Ellam, R.M., Hawkesworth, C.J., Menzies, M.A. and Rogers, N.W. (1989). The volcanism of Southern Italy: role of subduction and the relationship between potassic and sodic alkaline magmatism. *Journal of Geophysical Research* 94, 4589-4601.
- Ellam R.M., Harmon R.S., 1990. Oxygen isotope constraints on the crustal contributions to the subduction-related magmatism of the Aeolian Islands, Southern Italy. *J. Volcanol. Geotherm. Res.*, 44, 105-122.
- Esperanca S., Crisci G.M., De Rosa R., Mazzuoli R. (1992). The role of the crust in the magmatic evolution of the Island of Lipari. *Contrib. Mineral. Petrol.*, 112, 450-462.
- Francalanci, L., Barbieri, M., Manetti, P., Peccerillo, A. and Tolomeo, L. (1988). Sr-isotopic systematics in volcanic rocks from the Island of Stromboli (Aeolian arc). *Chemical Geology* 73, 164-180.
- Francalanci, L., Manetti, P. and Peccerillo, A. (1989). Volcanological and magmatological evolution of Stromboli volcano (Aeolian Islands): the roles of fractional crystallization, magma mixing, crustal contamination and source heterogeneity. *Bulletin of Volcanology* 51, 355-378.
- Francalanci, L., Manetti, P., Peccerillo A. and Keller, J. (1993). Magmatological evolution of the Stromboli volcano (Aeolian Arc, Italy): inferences from major and trace element and Sr-isotopic composition of lavas and pyroclastic rocks. *Acta Vulcanologica* 3, 127-151.
- Francalanci, L., Taylor, S.R., McCulloch, M.T., Woodhead, J. (1993). Geochemical and isotopic variations in the calc-alkaline rocks of the Aeolian Arc (Southern Italy): constraints on the magma genesis. *Contr. Mineral. Petrol.* (113), 300-313.
- Francalanci, L., Tommasini, S. and Conticelli, S. (2003). The volcanic activity of Stromboli in the 1906-1998 A.D. period: mineralogical, geochemical and isotope data relevant to the understanding of the plumbing system. *Journal of Volcanology and Geothermal Researches* in press.
- Francalanci, L., Tommasini, S., Conticelli, S. and Davies, G.R. (1999). Sr isotope evidence for short magma residence time for the 20th century activity at Stromboli volcano, Italy. *Earth Planetary Science Letters* 167, 61-69.
- Frazzetta, G., La Volpe, L. & Sheridan, M.F. (1983) Evolution of the Fossa Cone, Vulcano. *J. Volcanol. Geotherm. Res.*, 17, 329-360.
- Frazzetta, G., Gillot, P.Y., La Volpe, L. & Sheridan, M.F. (1984) Volcanic hazard at La Fossa of Vulcano: data from the last 6000 years. *Bull. Volcanol.*, 47, 105-124.
- Frazzetta G., La Volpe L. and Sheridan M.F. (1989). Interpretation of emplacement units in recent surge deposits on Lipari, Italy. *Journal of Volcanology and Geothermal Researches*, 37, 339-350.
- Gabbianelli G., Gillot P.Y., Lanzafame G., Romagnoli C., Rossi P.L., 1990. Tectonic and volcanic evolution of Panarea (Aeolian Islands, Italy). *Mar. Geol.*, 92, 313-326.

- Gabbianelli G., Romagnoli C., Rossi P.L., Calanchi N., 1993. Marine Geology of the panarea-Stromboli area (Aeolian Arcipelago, South-eastern Tyrrhenian sea). *Acta Vulcanol.*, 3, 11-20.
- Gamberi F., Marani M., Savelli C. (1997). Tectonic, volcanic and hydrothermal features of a submarine portion of the Aeolian arc (Tyrrhenian sea). *Marine Geology*, 140, 1-2, 167-181.
- Gertisser R., Keller J., 2000. From basalt to dacite: origin and evolution of the calc-alkaline series of Salina, Aeolian Arc, Italy. *Contrib. Mineral. Petrol.*, 139, 607-626.
- Ghisetti F. (1979). Relazioni tra strutture e fasi trascorrenti e distensive lungo i sistemi Messina-Fiumefreddo, Tindari-Letojanni e Alia-Malvagna (Sicilia nororientale): uno studio microtettonico. *Geol. Romana.*, 18, 23-58.
- Gioncada, A., Gurioli, L., & Sbrana, A. (1995) The hydrothermal-magmatic eruption of "Breccia di Commenda, La Fossa, Vulcano (Eolian Islands, Italy). *Per. Mineral.*, 64, 191-192.
- Gioncada A., Mazzuoli R., Bisson M., Pareschi M.T. (2003) Petrology of volcanic products younger than 42 ka on the Lipari-vulcano complex (Aeolian Islands, Italy): an example of volcanism controlled by tectonics. *Jour. Volcanol. Geotherm. Res.*, 122, 191-220.
- Giberti, G., Jaupart, C. and Sartoris, G. (1992). Steady-state operation of Stromboli volcano, Italy: constraints on the feeding system. *Bulletin of Volcanology* 54, 535-541.
- Gillot P.Y. (1987). Histoire volcanique des Iles Eoliennes: arc insulaire or complexe orogenique anulaire ?. *D.T. IGAL*, 11, 35-42.
- Gillot, P.Y. and Keller, J. (1993). Radiochronological dating of Stromboli. *Acta Vulcanologica* 3: 69-77.
- Harris, A.J.L. and Stevenson, D.S. (1997). Magma budgets and steady state activity of Vulcano and Stromboli. *Geophysical Research Letters* 24, 1043-1046.
- Hornig-Kjarsgaard, I., Keller, J., Koberski, U., Stadlbauer, E., Francalanci, L. and Lenhart, R. (1993). Geology, stratigraphy and volcanological evolution of the Island of Stromboli, Aeolian arc, Italy. *Acta Vulcanologica* 3, 21-68.
- Housh, T.B. and Luhr, J.F., 1991, Plagioclase-melt equilibria in hydrous systems. *American Mineralogist*, 76:477-492.
- Italiano F., Nuccio P.M., 1991. Geochemical investigations of submarine volcanic exhalations to the east of Panarea, Aeolian Islands, Italy. *J. Volcanol. Geotherm. Res.*, 46, 125-141.
- Jaupart C, Allègre CJ (1991) Gas content, eruption rate and instabilities of eruption regime in silicic volcanoes. *Earth Planet Sci Letters* 102: 413-429.
- Johannes W., Holtz F. (1996) Petrogenesis and experimental petrology of granitic rocks. *Springer Verlag*, 335 p.
- Keller J. (1982). Mediterranean island arcs. In Thorpe R.S. (Ed.) *Andesites*. *Wiley Chichester*, 307-325.
- Keller, J. (1980). The Island of Salina. *Rendiconti della Società Italiana di Mineralogia e Petrografia* 36, 489-524.
- Keller, J., Morche, W. (1993). Exceptional explosivity of Upper Quaternary andesitic volcanism of Salina, Aeolian Islands: dynamics of fall, surge and blast events. *IAVCEI General Assembly Canberra 1993*, Abstract Volume p.57.
- Lanzafame G. and Bousquet J.C. (1997). The Maltese escarpment and its extension from Mt. Etna to Aeolian Islands (Sicily): importance and evolution of a lithospheric discontinuity. *Acta Vulcanol.*, 9, 121-135.
- Losito R. (1989). Stratigrafia, caratteri deposizionali e aree sorgente dei tufi bruni delle Isole Eolie. *PhD Thesis*, Università di Bari, Italy.
- Luais, B. (1988). Mantle mixing and crustal contamination as the origin of the high-Sr radiogenic magmatism of Stromboli (Aeolian arc). *Earth Planetary Science Letters* 88, 93-106.
- Lucchi, F. (2000a). Evoluzione dell'attività vulcanica e mobilità verticale delle Isole Eolie nel tardo Quaternario. *PhD Thesis*, Università di Bologna, Italy.
- Lucchi, F. (2000b). Late Quaternary volcanic activity evolution and vertical mobility of the Aeolian Islands. *Plinius* 23, 101-107.
- Lucchi, F., Calanchi, N., Carobene, L., Tranne C.A. (1999). I terrazzi marini dell'Isola di Panarea (Isole Eolie): loro utilizzo nella definizione dell'eustatismo e del sollevamento tardo-Pleistocenico. *Bollettino della Società Geologica Italiana* 118, 545-562.
- Lucchi F., Tranne C.A., Calanchi N., Pirazzoli P.A., Romagnoli C., Radtke U., Reyss J.L., Rossi P.L. (2003). Late-Quaternary ancient shorelines at Lipari (Aeolian Islands): stratigraphical constraints to reconstruct geological evolution and vertical movements. *Quaternary International*, in press.

- Lucchi F., Tranne C.A., Calanchi N., Pirazzoli P.A., Romagnoli C., Rossi P.L. (2003). Late-Quaternary and recent sea-level changes and vertical displacements in the Aeolian Arc (Southern Tyrrhenian Sea). In: Riassunti e guida alle escursioni; workshop: "Il contributo dello studio delle antiche linee di riva alla comprensione della dinamica recente. Escursioni nello stretto di Messina". Messina 6-8 maggio 2003; 33-35.
- Lucchi F., Tranne C.A., Calanchi N., Rossi P.L. (2004). Geological cartography in volcanic areas: the case of Lipari (Aeolian Islands). In *Atlante di cartografia geologica*, Pasquarè G., Venturini C. (eds). Convegno Geologico Internazionale, Firenze 2004, in press.
- Marani M.P. and Trua T. (2002) Thermal constriction and slab tearing at the origin of a superinflated spreading ridge: Marsili volcano (tyrrhenian Sea). *Jour. Geoph. Res.*, 107, 10.1029/JB00285.
- Métrich N., Bertagnini A., Landi P. and Rosi, M. (2001). Crystallization driven by decompression and water loss at Stromboli volcano (Aeolian Islands, Italy). *Journal of Petrology* 42, 1471-1490.
- Nazzareni, S., Molin, G., Peccerillo, A., Zanazzi, P.F. (2001). Volcanological implications of crystal-chemical variations in clinopyroxenes from the Aeolian Arc, Southern Tyrrhenian Sea, Italy. *Bull. Volcanol.* (63), 73-82
- Pasquarè, G., Francalanci, L., Garduño, V.H. and Tibaldi, A. (1993). Structure and geologic evolution of the Stromboli volcano, Aeolian islands, Italy. *Acta Vulcanologica* 3, 79-89.
- Renzulli, A., Serri, G., Santi, P., Mattioli, M., Holm, P.M. (2001) Origin of high-silica liquids at Stromboli volcano (Aeolian Islands, Italy) inferred from crustal xenoliths, *Bull. Volcanol.* (62), Issue 6/7, pp 400-419.
- Romagnoli, C., Kokelaar, P., Rossi, P.L. and Sodi, A. (1993). The submarine extension of the Sciarra del Fuoco feature (Stromboli isl.): morphologic characterisation. *Acta Vulcanologica* 3, 91-98.
- Rosi, M. (1980). The Island of Stromboli. *Rendiconti Società Italiana Mineralogia e Petrologia* 36, 345-368.
- Rosi, M., Bertagnini, A. and Landi, P. (2000). Onset of the persistent activity at Stromboli volcano (Italy). *Bullettin of Volcanology* 62, 294-300.
- Rutherford MJ, Devine JD (1988) The May 18, 1980, eruption of Mount St. Helens. 3- Stability and chemistry of amphibole in the magma chamber. *J Geophys Res* 93: 11.949-11.959.
- Santo A., Chen Y., Clark A.H., Farrar E. and Tsegaye A. (1995).  $^{40}\text{Ar}/^{39}\text{Ar}$  ages of the Filicudi islan volcanics: implications for the volcanological history of the Aeolian Arc, Italy. *Acta Vulcanol.*, 7, 13-18.
- Savelli C. (2000). Two-stage progression of volcanism (8-0 Ma) in the central Mediterranean (southern Italy). *Jour. Of Geodynamics*, 31, 87-104.
- Sheridan, M.F., Frazzetta, G., La Volpe, L., 1987. Eruptive histories of Lipari and Vulcano, Italy, during the past 22.000 years. In: J.H. Fink (Editor), The emplacement of silicic domes and lava flows. *Geol. Soc. Am., Spec. Pap.* 212, 29-34.
- Tibaldi, A. (2001). Multiple sector collapses at Stromboli volcano, Italy: how they work. *Bullettin of Volcanology* 63 (2/3), 112-125.
- Tranne, C.A., Lucchi, F., Calanchi, N., Lanzafame, G., Rossi, P.L. (2002). Geological map of the Island of Lipari (Aeolian Islands). *L.A.C.*, Firenze.
- Vaggelli, G., Francalanci, L., Ruggieri, G. and Testi, S. (2003). Persistent polybaric rests of calc-alkaline magmas at Stromboli volcano, Italy: pressure data from fluid inclusions in restitic quartzite nodules. *Bullettin of Volcanology* 65, 385-404.
- Vai, G.B. (1996). Revisione critico-storica dei Piani marini del Quaternario. *Servizio Geologico d'Italia, Miscellanea*, Vol. 6. Istituto Poligrafico e Zecca dello Stato, Roma, 179 pp.
- Ventura G., Vilardo G., Milano G., Pino N. A. (1999). Relationships among crustal structure, volcanism and strike-slip tectonics in the Lipari-Vulcano volcanic complex (Aeolian Islands, Southern Tyrrhenian Sea, Italy). *Physics of the Earth and Planetary Interior*, 116, 31-52.
- Volpi V., Del Ben A., Martini F., Finetti I. (1997) Elaborazione ed Interpretazione della linea CROP-MARE 2A5 nel bacino di Gioia (Tirreno Sud-Orientale). *Proc. 16° Nat. Conv., GNGTS-CNR*, Cd-rom, 07.06
- Voltaggio, M., Branca, M., Tuccimei, P. & Tecce, F. (1995) Leaching procedure used in dating young potassic volcanic rocks by the  $^{226}\text{Ra}/^{230}\text{Th}$  method. *Earth Planet. Sc. Lett.*, 136, 123-131.
- Wang C.Y., Hwang W.T., Shi Y. (1989) Thermal evolution of a rift basin: the Tyrrhenian Sea. *Jour. Gephys. Res.*, 94, 3991-4006.

Wen, S. & Nekvasil H. (1994). "SOLVCALC: An interactive graphics program package for calculating the ternary feldspar solvus and for two feldspar geothermometry." *Computers & Geosciences* 20(No. 6): 1025-1040.

Woods AW, Koyaguchi T (1995) Transitions between explosive and effusive eruptions of silicic magmas. *Nature*, 370: 641-64

Back Cover:  
*field trip itinerary*

FIELD TRIP MAP

